On the Crucial Role of Antecedent–Consequent Structure Selection in LMI-Based PDC Control of TS Fuzzy Systems

Péter Baranyi

***Abstract*—This paper demonstrates that how the selection of antecedent–consequent structures in a TS fuzzy model plays a crucial role in the feasibility, conservativeness and optimality of Linear Matrix Inequality (LMI)-based Parallel Distributed Compensation (PDC) fuzzy control design. Specifically, the paper provides the first formal theoretical and necessity proofs that the resulting controller cannot be regarded as definitive or optimal until it is ensured that the best possible antecedent–consequent structure has been identified. The paper further proves that this sensitivity to the selection of the antecedent–consequent structure is an inherent and highly influential property of all qLPV systems. The practical implication of these results is that, systematically exploring antecedent–consequent structures may considerably improve the resulting control performance. This paper does not directly propose a new control design method. Instead, the mathematical framework developed in the proofs may serve as a first-order solution and as a foundation for future research on antecedent–consequent structure exploration strategies. To support the theoretical results, a comprehensive analysis of conceptual examples is presented that is well suited for geometric visualization and highlights the general occurrence and practical significance of the problem. In addition, a dynamically complex real-world engineering benchmark example is examined, demonstrating how exploring the antecedent–consequent structures leads to better solutions than those previously published.**

Keywords: TS fuzzy model, TS Fuzzy model transformation, TP model transformation, Parallel Distributed Compensation, Linear Matrix Inequalities, PDC, LMI, TS fuzzy control.

I. Introduction

The objective of this paper is to provide the first formal proof and to systematically demonstrate that the feasibility and optimality of Linear Matrix Inequality (LMI)-based Parallel Distributed Compensation (PDC) controller design framework [1], [2] critically depend on the selection of the antecedent fuzzy sets used in the underlying TS fuzzy model representation — a fundamental yet largely overlooked aspect of LMI-based PDC controller design and optimization framework.

This paper does not propose a new control design method; instead, it presents the mathematical framework developed for the proofs, which may serve as a first-order solution and as a starting point for future research aimed at systeematically exploring suitable antecedent–consequent structures to further improve LMI-based PDC control design.

In mainstream PDC control design, a TS fuzzy controller is derived from a TS fuzzy model representation of a given quasi–Linear Parameter-Varying state-space (qLPV) system, in which the controller and the TS fuzzy model share identical antecedent fuzzy sets. However, the derivation of the consequent control gains relies on LMIs constructed from the consequent systems of the TS fuzzy model; the antecedent fuzzy sets do not explicitly enter the LMI conditions. Consequently, the literature predominantly focuses on the selection and refinement of LMI conditions.

However, and this is the central point of the present work, any given qLPV state-space system admits infinitely many input–output equivalent TS fuzzy model representations that differ in their antecedent-consequent structure. Moreover, even for a fixed consequent system, infinitely many antecedent fuzzy set constructions can be defined, leading to a set of infinitely many TS fuzzy models whose controllability properties differ. As a consequence, a controller synthesized by substituting this fixed consequent system into the LMIs is optimized over the entire set of these TS fuzzy models, including those with the weakest controllability properties. This inherent set-based optimality is the fundamental reason why the LMI-based PDC control design framework is commonly characterized as conservative.

A. Motivation

The motivation of this paper is based on two key observations.

First, despite the significance of this issue, the systematic exploration or manipulation of antecedent–consequent structures has received little to no attention in the literature on LMI-based PDC control design frameworks. This is partly because the extent to which an inappropriate selection of antecedent-consequent structures can degrade the optimization capability of the applied LMIs is often underestimated, and partly because, deriving sequences of alternative TS fuzzy model representations in a systematic manner is not straightforward and, in general, no generic framework or procedure exists for doing so. As a result, it has remained unclear whether the additional effort required to derive alternative TS fuzzy model representations can yield substantial performance improvements. Even in the most recent publications employing LMI-based PDC frameworks, no systematic investigation

P. Baranyi (peter.baranyi@uni-corvinus.hu) is with the Corvinus Institute for Advanced Studies (CIAS) and Institute of Data Analytics and Information Systems at the Corvinus University of Budapest, Fővámtér 8, Budapest, Hungary and the Hungarian Research Network (HUN-REN). The author declares that there is no conflict of interest regarding the publication of this paper. The paper uses ChatBox App by Florate Ltd. to correct some texts of the paper.The research work was supported by National Research, Development and Innovation Office HURIZONT PROJECT 2025-2026 NKFIH - 2024-1.2.3-HU-RIZONT-2024-00030.

This article has been accepted for publication in IEEE Transactions on Fuzzy Systems. This is the author's version which has not been fully edited and content may change prior to final publication. Citation information: DOI 10.1109/TFUZZ.2026.3678634

can be found that examines whether alternative TS fuzzy model representations lead to improved control performance. Moreover, papers claiming optimal or best-achievable control solutions do not demonstrate that no alternative TS fuzzy model representation exists that could yield superior results.

Second, building upon the recently (2024) introduced extension of the TS fuzzy model transformation framework — namely, the TS fuzzy model transition theory [3] — it becomes possible, as introduced and exploited in this paper, to readily and systematically explore sequences of alternative input-output equivalent TS fuzzy model representations, and to rigorously analyze and formally prove the influence of antecedent–consequent structure manipulation on LMI feasibility and optimality.

B. Contributions and Novelty

This paper has two main contributions.

1) Fundamental theoretical contribution: The principal novel contribution of this paper is the provision of formal proofs of the following fundamental theorems: any given qLPV state-space system admits infinitely many input–output equivalent TS fuzzy model representations with different antecedent–consequent structures, among which there necessarily exist infinitely many representations that lead to infeasible LMIs, as well as infinitely many representations that yield feasible but highly suboptimal controllers and also representations that yield control solutions that are close to optimal or even optimal. Moreover, the proofs are constructive in the sense that the paper explicitly provides systematic procedures for constructing such infinitely many TS fuzzy model representations. Therefore, the proofs themselves constitute a first-order solution for systematic antecedent–consequent structure exploration, as demonstrated through both academic and real-world examples, where it is shown that this approach can lead to better solutions than those previously published.

While TS fuzzy model transformation–related studies have empirically observed performance variations [4]–[22] associated with different TS fuzzy model constructions, to the best of the authors' knowledge, there is no work in the literature that proves that the antecedent–consequent structure employed in such studies is optimal when "optimal" or "best" solutions are claimed. Further, no prior work has stated that, without such justification, claims of "optimal" or "best" solutions cannot be regarded as rigorously established. This paper closes this theoretical gap.

2) Illustrative and validation contribution: The paper also presents carefully constructed academic examples designed for illustration and supported by highly visualizable geometric representations. In addition, a real-world benchmark problem is examined. Together, these examples provide clear insight into the theoretical results and the main steps of the proofs, demonstrate their practical relevance, and show that the investigated phenomenon is not exceptional but rather a frequently occurring and practically significant issue that arises in typical modeling and control design scenarios.

In the real-world benchmark problem, we further demonstrate that better solutions than those previously published can be achieved through the antecedent–consequent structure exploration applied in the proof. This highlights the importance of the issue and shows why a "best" solution cannot be claimed unless it is verified that the appropriate antecedent–consequent structure has been selected.

C. Practical Implication

From a practical control design perspective, the above results indicate that antecedent–consequent structures derived from ad hoc constructions or standard methods — without considering the structural implications revealed in this paper — can lead to infeasible designs or to severe suboptimality of the resulting controller. Consequently, contrary to common practice in the literature, practical controller synthesis should not be considered complete once a TS fuzzy model has been constructed and the LMI-based PDC framework yields a controller. Instead, it should systematically explore alternative input–output equivalent TS fuzzy model representations in order to assess whether a more favorable representation exists that leads to improved control performance.

Therefore, the key practical implication is that achieving near-optimal or optimal control performance requires the joint consideration of the LMI formulation and the exploration of antecedent–consequent structures, rather than treating the TS fuzzy model structure as fixed.

D. Challenges and Core Idea of the Proof

To establish the proofs presented in this paper, we develop the Double TS fuzzy model transformation and transition, the novel analytical constructs introduced solely to enable the formal proofs presented herein. These constructions make it possible to represent a given qLPV system together with an arbitrarily selected non-controllable or marginally controllable variant of the same system by TS fuzzy models with identical consequent structures. As a result, the LMI-based PDC design no longer optimizes the controller solely for the original system, but instead jointly for both systems, which necessarily leads to infeasible or severely suboptimal solutions for the original system.

No transformation and transition methods of this type exist in the literature — in particular, none that is compatible with TS fuzzy model transitions. The development of such a transformation is a nontrivial task.

E. Structure of the paper

The structure of the paper is as follows. Apart from the Introduction and Conclusion, the paper can be conceptually divided into three main parts. Section II constitutes the first part and reviews all previously published concepts and methods that are utilized throughout the paper. The second part comprises Sections III–V and presents the novel contributions of the paper. The third part, Section VI, introduces a real-world benchmark example that investigates and illustrates these novel theoretical contributions.

The second part, which contains the novel contributions, is itself composed of three sections. First, Section III introduces

This article has been accepted for publication in IEEE Transactions on Fuzzy Systems. This is the author's version which has not been fully edited and content may change prior to final publication. Citation information: DOI 10.1109/TFUZZ.2026.3678634

two proof-enabling tools required for the subsequent theoretical developments. Next, the two main theorems of the paper are presented in Sections IV and V, respectively. Section IV focuses on infeasibility, while Section V addresses the case of feasible but suboptimal solutions. Both Sections IV and V follow the same structure: each begins with a formal theorem, followed by a discussion of its practical implications. This is then followed by the formal proof and, finally, by an illustrative example. These examples geometrically visualize the individual steps of the proofs and simultaneously demonstrate the associated practical implications.

II. Preliminary Concepts

The following notation is used in the paper:

- Indices are denoted by $i, j, k, l, n \dots$ with corresponding upper bounds denoted as $I, J, KL, N \dots$ respectively.
- Scalars, vectors, matrices and tensors (multidimensional matrix) are denoted as $s \in \mathbb{R}$, $\mathbf{s} \in \mathbb{R}^J$, $\mathbf{S} \in \mathbb{R}^{J_1 \times J_2}$, $\mathcal{S} \in \mathbb{R}^{J^N}$. E.g. notation $\mathcal{S} \in \mathbb{R}^{I^N \times J^2}$ is equivalent to $\mathcal{S} \in \mathbb{R}^{I_1 \times I_2 \times \dots I_N \times J_1 \times J_2}$.
- $[\mathcal{S}]_{index}$ addresses elements, e.g. $[\mathcal{S}]_{i_1,i_2,\dots i_N} = \mathbf{S}_{i_1,i_2,\dots i_N} \in \mathbb{R}^{J^2}$ of $\mathcal{S} \in \mathbb{R}^{I^N \times J^2}$;
- $[\mathcal{S}]_{index_1/index_2}$ is a vector containing the indexed elements as $\begin{bmatrix}[\mathcal{S}]_{index_1} & [\mathcal{S}]_{index_2}\end{bmatrix}$;
- $\Omega \subset \mathbb{R}^N$ denotes a domain defined as the Cartesian product of one-dimensional intervals $\omega_n = [\omega_n^{min}, \omega_n^{max}] \subset \mathbb{R}$, i.e., $\Omega = \omega_1 \times \ldots \times \omega_N$.
- $\Omega + \Delta$ denotes the domain obtained by shifting each interval ω_n of Ω by the element $[\Delta]_n$ of vector $\Delta \in \mathbb{R}^N$. That is for $\forall n : \omega_n + [\Delta]_n = [\omega_n^{min} + [\Delta]_n, \omega_n^{max} + [\Delta]_n]$.
- $w_i(p)$, $v_i(p)$ and $h_i(p)$ denote membership functions of Ruspini-partitioned fuzzy sets. In general, we use $\mu_i(p)$ to denote any of these; they satisfy $\forall p : \sum_{i=1}^{I} \mu_i(p) = 1$ and $\forall i, p : 0 \leq \mu_i(p)$.
- The symbolic notation $\{A, B, \dots\} \xrightarrow[Type]{Name} \{C, D, \dots\}$ denotes the application of a construction. The left-hand side represents the given entities, while the right-hand side represents the resulting entities. The superscript "Name" specifies the name of the construction, and the subscript "Type" denotes the selected type of the result.

In the next the fundamental concepts employed in this paper are presented, as outlined in the relevant literature.

Definition 1: **qLPV state-space system structure**

The paper defines the qLPV state-space system and controller as:

$$\begin{bmatrix}\dot{\mathbf{x}}(t) \\ \mathbf{y}(t)\end{bmatrix} = \mathbf{S}(\mathbf{p}(t)) \begin{bmatrix}\mathbf{x}(t) \\ \mathbf{u}(t)\end{bmatrix} \text{ and } \mathbf{u}(t) = -\mathbf{F}(\mathbf{p}(t))\mathbf{x}(t), \quad (1)$$

where $\mathbf{x}(t) \in \mathbb{R}^a$, $\mathbf{y}(t) \in \mathbb{R}^c$ and $\mathbf{u}(t) \in \mathbb{R}^b$ are the state, output and control vectors, respectively. $\mathbf{S}(\mathbf{p}(t)) \in \mathbb{R}^{J^2}$ is the parameter varying system matrix, and parameter vector $\mathbf{p}(t) \in \Omega \subset \mathbb{R}^N$ may contain elements of $\mathbf{x}(t)$. $\mathbf{F}(\mathbf{p}(t)) \in \mathbb{R}^{b \times a}$ determines the parameter dependent feedback gains of the controller. Submatrix $\mathbf{B}(\mathbf{p}(t)) = [\mathbf{S}(\mathbf{p}(t))]_{(1:J_1) \times (a+1:J_2)} \in \mathbb{R}^{J_1 \times b}$, is the input gain matrix of the system. For simplicity, we will omit time t from this point forward.

Here, we define the most commonly applied type of TS fuzzy model used in fuzzy control theory, as outlined in [1]:

Definition 2: **The TS Fuzzy model**

Consider a set of fuzzy rules in the form:

$$\text{IF } A_{1,i_1} \text{ AND } A_{2,i_2} \dots \text{AND } A_{N,i_N} \text{ THEN } \mathbf{S}_{i_1,i_2,\dots i_N}. \quad (2)$$

where the antecedent fuzzy sets A_{n,i_n} are defined by Ruspini-partitioned membership functions $w_{n,i_n}(p_n)$. The consequents are linear time and parameter invariant system matrices $\mathbf{S}_{i_1,i_2,\dots i_N} \in \mathbb{R}^{J^2}$ which are also referred to as vertex systems, consequent vertices or simply vertices. If the observation fuzzy sets are singletons located at p_n and the product-sum-gravity inference operator is used, then the transfer function of the TS fuzzy model takes the following form [4], [23]–[25]:

$$\mathbf{S}(\mathbf{p}) = \sum_{i_1}^{I_1} \sum_{i_2}^{I_2} \dots \sum_{i_N}^{I_N} \prod_{n=1}^{N} w_{n,i_n}(p_n) \mathbf{S}_{i_1,i_2,\dots i_N}. \quad (3)$$

An important property of Eq. (3) is that, for any input $\mathbf{p}$, the output remains within the convex hull defined by the vertices: $\mathbf{S}(\mathbf{p}) \in co\{\mathbf{S}_{i_1,i_2,\dots i_N}\}$ — guaranteed by the Ruspini-partition of all $w_{n,i}(p_n)$.

The transfer function in Eq. (3), formulated using vector–tensor product operations — first introduced in tensor (multidimensional matrix) algebra in 2000 [26] and subsequently used extensively in the TS fuzzy model transformation literature [3], [4], [24], [25], [27]–[31] — takes the following form [4], [24], [25]:

$$\mathbf{S}(\mathbf{p}) = \mathcal{S} \mathop{\boxtimes}_{n=1}^{N} \mathbf{w}_n(p_n), \quad (4)$$

where the antecedents are collected in vector $\mathbf{w}_n(p_n) = \begin{bmatrix}w_{n,1}(p_n) & w_{n,2}(p_n) \dots w_{n,I_N}(p_n)\end{bmatrix} \in \mathbb{R}^{I_n}$ which is referred to as the antecedent system, and vertices $\mathbf{S}_{i_1,i_2,\dots i_N}$ are stored in a tensor $\mathcal{S} \in \mathbb{R}^{I^N \times J^2}$ that is referred to as the consequent system. The operator $\boxtimes$ defines the rule-based mapping between antecedents and consequents according to Eq. (2). Note that the operator $\boxtimes$ in Eq. (4) is mathematically equivalent to the sum–product operation in Eq. (3), while offering a more compact notation. In fact, the definition of the $\boxtimes$ operator is precisely the multi–sum–product operation given in Eq. (3). If the reader is not familiar with the vector–tensor product, Eq. (4) may simply be regarded as a concise symbolic notation of the TS fuzzy model; alternatively, see, for example, any of Chapter 2 of [24], Chapter 3 of [25] for concise and self-contained descriptions.

The proofs in the paper are based on the TS fuzzy model transformation. Its related literature is vast and extensive, see some key publications [3], [4], [24], [25], [27]–[31]. In the following, we summarize the aspects most relevant to the present study as follows.

Method 1: **TS fuzzy model transformation**

The TS fuzzy model transformation [4], [24], [25] converts a given system matrix $\mathbf{S}(\mathbf{p}) \in \mathbb{R}^{J^2}$ of Eq. (1) into the TS fuzzy model form of Eq. (4). It derives the antecedent systems $\mathbf{w}_n(p_n)$ and the consequent system $\mathcal{S}$ to a given $\mathbf{S}(\mathbf{p})$. We introduce the following symbolic notation:

$$\{\mathbf{S}(\mathbf{p})\} \xrightarrow[\text{Type}]{\text{TS Transformation}} \{\mathcal{S},\ \mathbf{w}_n(p_n)\}, \quad (5)$$

This article has been accepted for publication in IEEE Transactions on Fuzzy Systems. This is the author's version which has not been fully edited and content may change prior to final publication. Citation information: DOI 10.1109/TFUZZ.2026.3678634

where Type $\in \{\mathrm{CNO}, \mathrm{IRNO}, \mathrm{SNNN}\}$, as discussed below. The most important properties to highlight in the present case are as follows:

i) The transformation determines the minimal number of antecedents per input (i.e., I_n is minimized), resulting in the minimal number of consequent vertices [3], [4], [24], [25], [27]–[31].

ii) It can construct several useful types of antecedent systems $\mathbf{w}_n(p_n)$, such as Sum Normalized and Non-Negative (SNNN), Close to Normalized (CNO), and Inverse Relaxed Normalized (IRNO) types, leading to different convex hulls defined by the vertices $[\mathcal{S}]_{i_1,i_2,\ldots i_N}$.

The SNNN-type antecedent system is designed solely to satisfy the Ruspini partition property and does not aim to achieve any additional structural objectives. In contrast, the CNO and IRNO types — as special cases or refinements of the SNNN — were originally designed to yield more linguistically interpretable (normalised) fuzzy sets. Later, the ability of CNO to produce a tighter convex hull of the vertices also gained attention.For further mathematical details on deriving SNNN-, CNO-, and IRNO-type antecedents, the interested reader is referred to [24], [32]; however, this mathematical depth is not required for understanding the use of SNNN, CNO, and IRNO types in the present paper. Throughout this paper, TS fuzzy models and their corresponding convex hulls are termed CNO, IRNO, or SNNN types whenever they are constructed using antecedent fuzzy sets of the respective type.

iii) Not all functions $\mathbf{S}(\mathbf{p})$ admit an exact representation in the form of Eq. (3) or Eq. (4) when the indices I_n are bounded [33]. However, in such cases, by increasing I_n toward infinity, an approximation error can be achieved that is arbitrarily small and, in practice, significantly smaller than the typical system identification error. Therefore, throughout this paper, the theory is presented as if an exact TS fuzzy model of the given system $\mathbf{S}(\mathbf{p})$ always exists. If an exact TS fuzzy model representation does not exist, $\mathbf{S}(\mathbf{p})$ is replaced by a closest variant (that has exact TS fuzzy model representation) that differs from $\mathbf{S}(\mathbf{p})$ only by a negligibly small error — essentially of numerical magnitude — or, at least, by an error that is substantially smaller than the identification uncertainty. In this sense, this variant can equivalently be regarded as the outcome of the system identification process. Note that the TS fuzzy model transformation automatically identifies such a closest variant, with an arbitrarily small approximation error. Accordingly, in this paper we assume that $\mathbf{S}(\mathbf{p})$ admit an exact decomposition. Note that the models used in the examples indeed possess exact TS fuzzy representations.

Method 2: **Pseudo TS fuzzy model transformation**

The Pseudo TS fuzzy model transformation, published in [3], [4], [24], [25], [27]–[31], is considered the pseudo inverse of the TS fuzzy model transformation in that it derives the consequents in $\mathcal{S}$ of TS fuzzy model Eq. (4) for a given $\mathbf{S}(\mathbf{p})$ and specified antecedent system $\mathbf{w}_n(p_n)$. Let us use the following symbolic notation:

$$\{\mathbf{S}(\mathbf{p}), \mathbf{w}_n(p_n)\} \xrightarrow{\text{Pseudo TS Transformation}} \{\mathcal{S}\}. \tag{6}$$

Note that the weighting functions $\mathbf{w}_n(p_n)$ must ensure sufficient rank; otherwise, only an approximate representation can be obtained. In the present paper, all weighting functions $\mathbf{w}_n(p_n)$ satisfy this rank condition.

The paper also utilizes the recently published (in 2024) TS fuzzy model transition method [3].

Method 3: **TS fuzzy model transition**

the TS fuzzy model transition let us define the following symbolic notation as:

$$\{\mathcal{S}^1, \mathbf{w}_n^1(p_n), \mathcal{S}^2, \mathbf{w}_n^2(p_n), \lambda\} \xrightarrow{\text{TS Transition}} \{\mathcal{S}^\lambda, \mathbf{w}_n^\lambda(p_n)\}. \tag{7}$$

Consider two alternative TS fuzzy model variants of $\mathbf{S}(\mathbf{p})$ derived via TS fuzzy model transformation (in both cases, the same value of I_n is set for all n), for instance, one of CNO type and the other of SNNN type:

$$\{\mathbf{S}(\mathbf{p})\} \xrightarrow[\text{Type 1}]{\text{TS Transformation}} \{\mathcal{S}^1, \mathbf{w}_n^1(p_n)\} \tag{8}$$

$$\{\mathbf{S}(\mathbf{p})\} \xrightarrow[\text{Type 2}]{\text{TS Transformation}} \{\mathcal{S}^2, \mathbf{w}_n^2(p_n)\} \tag{9}$$

that results in

$$\mathbf{S}(\mathbf{p}) = \mathcal{S}^1 \mathop{\boxtimes}_{n=1}^{N} \mathbf{w}_n^1(p_n) = \mathcal{S}^2 \mathop{\boxtimes}_{n=1}^{N} \mathbf{w}_n^2(p_n). \tag{10}$$

The TS fuzzy model transition defines a TS fuzzy model

$$\mathbf{S}(\mathbf{p}) = \mathcal{S}^\lambda \mathop{\boxtimes}_{n=1}^{N} \mathbf{w}_n^\lambda(p_n), \tag{11}$$

where the antecedents, denoted by superscript λ, are interpolated as

$$\mathbf{w}_n^\lambda(p_n) = (1-\lambda)\mathbf{w}_n^1(p_n) + \lambda \mathbf{w}_n^2(p_n)\mathbf{Z}_n \tag{12}$$

on all dimensions of $\mathbf{p}$, where $\lambda \in [0,1]$ represents the transition parameter. $\mathbf{Z}_n$ determines between which membership functions the interpolation takes place, so as it defines the interpolation pairs of the membership functions in $\mathbf{w}_n^1(p_n)$ and $\mathbf{w}_n^2(p_n)$. The consequent vertices, stored in $\mathcal{S}^\lambda$ are determined to $\mathbf{S}(\mathbf{p})$ and the interpolated $\mathbf{w}_n^\lambda(p_n)$ by the Pseudo TS fuzzy model transformation (Method 2) as $\{\mathbf{S}(\mathbf{p}), \mathbf{w}_n^\lambda(p_n)\} \xrightarrow{\text{Pseudo TS Transformation}} \{\mathcal{S}^\lambda\}$.

As a result, the consequent vertices in $\mathcal{S}^\lambda$ transition between the corresponding vertices stored in $\mathcal{S}^1$ and $\mathcal{S}^2$. The paper introducing the TS fuzzy model transition [3] shows that the choice of the matrix $\mathbf{Z}$ can result in either jarring or smooth transitions. In the present paper, we assume that $\mathbf{Z}_n$ is always chosen such that it yields smooth transitions, therefore, in the following we omit $\mathbf{Z}_n$ from the discussion and from the symbolic notations, since it has no relevance for the purposes of the present paper.

In the following, we review the framework of the PDC control design as presented in [1].

Framework 1: **LMI-based PDC control design**

This framework assumes that the TS fuzzy model (Eq. (4)) of $\mathbf{S}(\mathbf{p})$ is provided, and the goal is to control $\mathbf{x} \to \mathbf{0}$. It then derives the controller, defined in Eq. (1), in TS fuzzy model form as:

$$\mathbf{F}(\mathbf{p}) = \mathcal{F} \mathop{\boxtimes}_{n=1}^{N} \mathbf{w}_n(p_n), \tag{13}$$

This article has been accepted for publication in IEEE Transactions on Fuzzy Systems. This is the author's version which has not been fully edited and content may change prior to final publication. Citation information: DOI 10.1109/TFUZZ.2026.3678634

where the antecedent system $\mathbf{w}_n(p_n)$ of the controller is inherited from the given TS fuzzy model (Eq. (4)), and the vertices $[\mathcal{F}]_{i_1,i_2,...i_N}$ are derived by LMIs from the vertices $[\mathcal{S}]_{i_1,i_2,...i_N}$. There exists a wide variety of LMIs, each with distinct properties that aid in optimizing control performance [2]. For this framework let us use the symbolic expression as

$$\{\mathcal{S}\} \xrightarrow{LMI} \{\mathcal{F}\}. \tag{14}$$

The above LMI-based PDC design Framework 1 is considered conservative and may not always lead to feasible LMIs. Let us recall the following property [1], [2]:

Property 1: **Infeasible LMIs - suboptimal result**

It is important to emphasize that

A) if there exists $\mathbf{p}$ such that $\mathbf{S}(\mathbf{p})$ is not controllable, then the consequent vertex systems $[\mathcal{S}]_{i_1,i_2,...i_N}$ of any TS fuzzy model representation of $\mathbf{S}(\mathbf{p}) = \mathcal{S} \boxtimes_{n=1}^{N} \mathbf{w}_n(p_n)$ necessarily lead to infeasible LMIs.

B) even in case the system $\mathbf{S}(\mathbf{p}) = \mathcal{S} \boxtimes_{n=1}^{N} \mathbf{w}_n(p_n)$ is controllable for all $\mathbf{p}$ and all the vertices $[\mathcal{S}]_{i_1,i_2,...i_N}$ are themselves controllable, the LMIs executed on $[\mathcal{S}]_{i_1,i_2,...i_N}$ are not feasible whenever there exists a convex combination of this vertex system that defines a non-controllable system, i.e. there exist non-controllable systems (denoted by the superscript "nc") of the form $\mathbf{S}^{nc}(\mathbf{p}) = \mathcal{S} \boxtimes_{n=1}^{N} \mathbf{v}_n(p_n)$.

C) when there are two controllable system $\mathbf{S}^A(\mathbf{p}) = \mathcal{S} \boxtimes_{n=1}^{N} \mathbf{w}_n(p_n)$ and $\mathbf{S}^B(\mathbf{p}) = \mathcal{S} \boxtimes_{n=1}^{N} \mathbf{v}_n(p_n)$ that share the same vertices, the LMIs in Eq. (14) yield a vertex system $\mathcal{F}$ that is optimized simultaneously for both systems, and is therefore not individually optimal for either system alone. In practice, this is often expressed by stating that the LMI-based design is performed for the worst-case system, that is, for the weakest controllable system within the convex hull defined by the vertices.

For simplicity, in the examples presented in this paper, we employ a basic LMI condition for PDC control design, taken from [1] (page 58) and recalled below:

Framework 2: **Asymptotically stable controller**

Consider a system matrix model $\mathbf{S}(\mathbf{p}) = \sum_{i=1}^{I} w_i(\mathbf{p})\mathbf{S}_i$, with controller feedback gain $\mathbf{F}(\mathbf{p}) = \sum_{i=1}^{I} w_i(\mathbf{p})\mathbf{F}_i$, where the vertices of the model are partitioned as $\mathbf{S}_i = \begin{bmatrix}\mathbf{A}_i \in \mathbb{R}^{a\times a} & \mathbf{B}_i \in \mathbb{R}^{a\times b}\end{bmatrix}$. This control structure is globally and asymptotically stable if there exist $\mathbf{P} > 0$ and $\mathbf{M}_i$ satisfying equations

$$-\mathbf{P}\mathbf{A}_i^T - \mathbf{A}_i\mathbf{P} + \mathbf{M}_i^T\mathbf{B}_i^T + \mathbf{B}_i\mathbf{M}_i > 0, \tag{15}$$

$$-\mathbf{P}\mathbf{A}_i^T - \mathbf{A}_i\mathbf{P} - \mathbf{P}\mathbf{A}_s^T - \mathbf{A}_s\mathbf{P} + \mathbf{M}_s^T\mathbf{B}_i^T + \mathbf{B}_i\mathbf{M}_s + \mathbf{M}_i^T\mathbf{B}_s^T + \tag{16}$$

$$+\mathbf{B}_s\mathbf{M}_i \geq 0, \tag{17}$$

for all $i < s \leq I$, such that $w_i(\mathbf{p})w_s(\mathbf{p}) \neq 0$. The feedback gains are then obtained as $\mathbf{F}_i = \mathbf{M}_i\mathbf{P}^{-1}$.

III. Proof-Enabling Concepts: Double TS Fuzzy Model Transformation and transition

The proofs presented in Section IV and V rely on the Double TS fuzzy model transformation (Method 4) and transition (Method 5) developed in this section. For clarity and ease of understanding, these Methods are introduced here solely as auxiliary tools supporting the subsequent theoretical derivations.

Method 4: **Double TS fuzzy model transformation**

Consider two systems $\mathbf{S}^A(\mathbf{p}), \mathbf{S}^B(\mathbf{p}) \in \mathbb{R}^{J^2}$. The goal is to transform both to TS fuzzy model representations as

$$\mathbf{S}^A(\mathbf{p}) = \mathcal{S} \boxtimes_{n=1}^{N} \mathbf{w}_n(p_n) \text{ and } \mathbf{S}^B(\mathbf{p}) = \mathcal{S} \boxtimes_{n=1}^{N} \mathbf{v}(p_n), \tag{18}$$

which share the same consequents stored in $\mathcal{S}$. Let us define the symbolic notation as:

$$\{\mathbf{S}^A(\mathbf{p}), \mathbf{S}^B(\mathbf{p})\} \xrightarrow[Type]{\text{Double TS Transformation}} \{\mathcal{S}, \mathbf{w}_n(p_n), \mathbf{v}_n(p_n)\}, \tag{19}$$

where $Type \in \{SNNN, CNO, IRNO\}$. The method has the following steps:

Step 1: Merging the systems: Define the matrix function $\mathbf{H}(\mathbf{p}')$ for $\mathbf{p}' \in \Omega'$ by aligning $\mathbf{S}^A(\mathbf{p})$ and the shifted variant of $\mathbf{S}^B(\mathbf{p})$ as

$$\mathbf{H}(\mathbf{p}') = \begin{cases} \mathbf{S}^A(\mathbf{p}') & \text{if } \mathbf{p}' \in \Omega \\ \mathbf{S}^B(\mathbf{p}' - \Delta) & \text{if } \mathbf{p}' \in \Omega + \Delta \end{cases}, \tag{20}$$

where $\Omega' = \Omega \cup (\Omega + \Delta)$. We execute the alignment along a single, arbitrarily selected dimension z of $\mathbf{p}$ by choosing $[\Delta]_z > \omega_z^{\max} - \omega_z^{\min}$ (to guarantee $\Omega \cap (\Omega + \Delta) = \emptyset$ as required by Eq. (20)) and let $[\Delta]_n = 0$ for all $n \neq z$.

Step 2: TS fuzzy model transformation: Execute the TS fuzzy model transformation (Method 1) on $\mathbf{H}(\mathbf{p}')$ as $\{\mathbf{H}(\mathbf{p}')\} \xrightarrow[Type]{\text{TS Transformation}} \{\mathcal{S}, \mathbf{h}_n(p_n)\}$, that results in

$$\mathbf{H}(\mathbf{p}') = \mathcal{S} \boxtimes_{n=1}^{N} \mathbf{h}_n(p_n'), \tag{21}$$

The resulting $\mathcal{S}$ here is ready for use in Eq. (18) and (19).

Step 3: Separation: In the same way as the systems $\mathbf{S}^A(\mathbf{p})$ and $\mathbf{S}^B(\mathbf{p})$ were aligned along the z-th dimension, the resulting TS fuzzy model in Eq. (21) can also be separated along that dimension. Accordingly, the corresponding antecedent fuzzy sets $\mathbf{h}_n(p_n')$ are separated and shifted back to their original interval in this step. Based on construction in Eq. (20) we have

$$\mathbf{S}^A(\mathbf{p}) = \mathbf{H}(\mathbf{p}) \text{ and } \mathbf{S}^B(\mathbf{p}) = \mathbf{H}(\mathbf{p} + \Delta). \tag{22}$$

It follows that $\mathbf{w}_n(p_n)$ and $\mathbf{v}_n(p_n)$ of Eq. (18) are defined by

$$\mathbf{w}_n(p_n) = \mathbf{h}_n(p_n) \text{ and } \mathbf{v}_n(p_n) = \mathbf{h}_n(p_n + \Delta_n). \tag{23}$$

Although not essential for the purposes of this paper, we note that $\mathbf{w}_n(p_n)$ and $\mathbf{v}_n(p_n)$ differ only in the z-th dimension.

Method 5: **Double TS fuzzy model transition**

This article has been accepted for publication in IEEE Transactions on Fuzzy Systems. This is the author's version which has not been fully edited and content may change prior to final publication. Citation information: DOI 10.1109/TFUZZ.2026.3678634

Let us define the following symbolic notation for this objective:

$$\{\mathbf{S}^A(\mathbf{p}),\mathbf{S}^B(\mathbf{p}),\lambda\} \xrightarrow[Type1,Type2]{\text{Double TS Transition}} \{\mathcal{S}^\lambda,\mathbf{w}_n^\lambda(p_n),\mathbf{v}_n^\lambda(p_n)\}, \tag{24}$$

where $Type1, Type2 \in \{SNNN, CNO, IRNO\}$, $Type1 \neq Type2$.

This method incorporates the TS fuzzy model transition (Method 3) into the Double TS fuzzy model transformation (Method 4). Consider the given $\mathbf{S}^A(\mathbf{p})$ and $\mathbf{S}^B(\mathbf{p})$. The objective is to derive two distinct TS fuzzy model representations of $\mathbf{S}^A(\mathbf{p})$ as

$$\mathbf{S}^A(\mathbf{p}) = \mathcal{S}^{Type1} \underset{n=1}{\overset{N}{\boxtimes}} \mathbf{w}_n^{Type1}(p_n) = \mathcal{S}^{Type2} \underset{n=1}{\overset{N}{\boxtimes}} \mathbf{w}_n^{Type2}(p_n), \tag{25}$$

and the transition between them as

$$\{\mathcal{S}^{Type1},\mathbf{w}_n^{Type1}(p_n),\mathcal{S}^{Type2},\mathbf{w}_n^{Type2}(p_n),\lambda\} \xrightarrow{\text{TS Transition}} \{\mathcal{S}^\lambda,\mathbf{w}_n^\lambda(p_n)\} \tag{26}$$

leading to

$$\mathbf{S}^A(\mathbf{p}) = \mathcal{S}^\lambda \underset{n=1}{\overset{N}{\boxtimes}} \mathbf{w}_n^\lambda(p_n), \tag{27}$$

with a very important constrain that all representations are constructed such that there exists a convex combination - defined by $\mathbf{v}_n(p_n)$ - of their consequent vertices that defines the given $\mathbf{S}^B(\mathbf{p})$ as

$$\mathbf{S}^B(\mathbf{p}) = \mathcal{S}^\lambda \underset{n=1}{\overset{N}{\boxtimes}} \mathbf{v}_n^\lambda(p_n). \tag{28}$$

The method proceeds in the following steps:

Step 1: This step executes the Step 1 of the Double TS fuzzy model transformation (Method 4) to define $\mathbf{H}(\mathbf{p}')$ by merging $\mathbf{S}^A(\mathbf{p})$ and $\mathbf{S}^B(\mathbf{p})$, see Eq. (20). Then execute Step 2 of the Double TS fuzzy model transformation (Method 4) two times to derive two different (for instance one CNO and one SNNN type) TS fuzzy models of $\mathbf{H}(\mathbf{p}')$ as:

$$\{\mathbf{H}(\mathbf{p}')\} \xrightarrow[Type1]{\text{TS Transformation}} \{\mathcal{S}^1,\mathbf{h}_n^1(p_n)\} \tag{29}$$

$$\{\mathbf{H}(\mathbf{p}')\} \xrightarrow[Type2]{\text{TS Transformation}} \{\mathcal{S}^2,\mathbf{h}_n^2(p_n)\}, \tag{30}$$

that results in

$$\mathbf{H}(\mathbf{p}') = \mathcal{S}^1 \underset{n=1}{\overset{N}{\boxtimes}} \mathbf{h}_n^1(p_n') = \mathcal{S}^2 \underset{n=1}{\overset{N}{\boxtimes}} \mathbf{h}_n^2(p_n'). \tag{31}$$

Step 2: This step employs the TS fuzzy model transition method (Method 3) to establish the smooth transition between the TS fuzzy models derived in the preceding step as

$$\{\mathcal{S}^1,\mathbf{h}_n^1(p_n),\mathcal{S}^2,\mathbf{h}_n^2(p_n),\lambda\} \xrightarrow{\text{TS Transition}} \{\mathcal{S}^\lambda,\mathbf{h}_n^\lambda(p_n)\} \tag{32}$$

that results in

$$\mathbf{H}(\mathbf{p}') = \mathcal{S}^\lambda \underset{n=1}{\overset{N}{\boxtimes}} \mathbf{h}_n^\lambda(p_n'), \tag{33}$$

see Eq. (11) of Method 3).

Step 3: This step is identical to Step 3 of the Double TS fuzzy model transformation (Method 4). It separates $\mathbf{h}_n^\lambda(p_n')$ of Eq. (33) - according to Eq. (22) and (23) - that results in $\mathbf{w}_n^\lambda(p_n)$ and $\mathbf{v}_n^\lambda(p_n)$. Thus finally we have the two TS fuzzy model representations sharing the same consequent system $\mathbf{S}^\lambda$ as:

$$\mathbf{S}^A(\mathbf{p}) = \mathcal{S}^\lambda \underset{n=1}{\overset{N}{\boxtimes}} \mathbf{w}_n^\lambda(p_n) \text{ and } \mathbf{S}^B(\mathbf{p}) = \mathcal{S}^\lambda \underset{n=1}{\overset{N}{\boxtimes}} \mathbf{v}_n^\lambda(p_n). \tag{34}$$

IV. Infeasible LMI-Based PDC Design

A. Theorems

Theorem 1: Every $\mathbf{S}(\mathbf{p})$, that is controllable for all $\mathbf{p}$ has an infinite number of input-output equivalent TS fuzzy model representations, where the consequent vertices lead to infeasible LMIs in the PDC design Framework 1.

Practical Implication 1: When deriving a TS fuzzy model with arbitrarily chosen antecedent fuzzy sets, one can easily encounter situations in which the resulting consequent vertices lead to infeasible LMIs, even when the given system and the vertices of the resulting TS fuzzy model are controllable. This also means that, in such cases, instead of modifying the applied LMIs, exploring alternative TS fuzzy model representations may restore feasibility.

The following Lemma 1 formalizes the key claim underlying Theorem 1. Its proof, together with Property 1, establishes Theorem 1. Let $\mathbf{S}^{nc}(\mathbf{p}) \in \mathbb{R}^{J^2}$ (where $\mathbf{x} \in \mathbb{R}^a$) be a non-controllable system i.e., a system for which there exists at least one $\mathbf{p}$ such that controllability is violated.

Lemma 1: For any given system $\mathbf{S}(\mathbf{p})$, there exist infinitely many TS fuzzy model representations

$$\mathbf{S}(\mathbf{p}) = \mathcal{S}^k \underset{n=1}{\overset{N}{\boxtimes}} \mathbf{w}_n^k(p_n), \text{ where } k = 1,\ldots,K=\infty, \tag{35}$$

whose consequent vertices stored in $\mathcal{S}^k$ define a convex hull that contains at least one non-controllable system as $\mathbf{S}^{nc}(\mathbf{p})$. Consequently, there exist antecedent fuzzy set systems $\mathbf{v}_n^k(p_n)$ that define TS fuzzy model representations of $\mathbf{S}^{nc}(\mathbf{p})$ as

$$\mathbf{S}^{nc}(\mathbf{p}) = \mathcal{S}^k \underset{n=1}{\overset{N}{\boxtimes}} \mathbf{v}_n^k(p_n). \tag{36}$$

B. Proof of the Theorem 1 and Lemma 1

The proof is constructive in nature: we explicitly demonstrate how, for a given system matrix $\mathbf{S}(\mathbf{p})$, infinitely many TS fuzzy model representations can be constructed whose consequent vertices are also the consequent vertices of a TS fuzzy model representation of a non-controllable system $\mathbf{S}^{nc}(\mathbf{p})$. In other words, these consequent vertices define a convex hull that contains the non-controllable system $\mathbf{S}^{nc}(\mathbf{p})$. The steps of the construction are as follows.

Step 1: First of all let us define an $\mathbf{S}^{nc}(\mathbf{p})$.

Proposition 1: A non-controllable system $\mathbf{S}^{nc}(\mathbf{p})$ can always be constructed from a given system $\mathbf{S}(\mathbf{p})$ in many different ways. For illustration, we mention two simple possibilities. One option is to set the input matrix block $\mathbf{B}(\mathbf{p})$ of the system $\mathbf{S}(\mathbf{p})$ to the zero matrix. Alternatively, any z-th row, z = 1, . . . , a, of $\mathbf{S}(\mathbf{p})$ can be replaced by the corresponding row of the identity matrix.

This article has been accepted for publication in IEEE Transactions on Fuzzy Systems. This is the author's version which has not been fully edited and content may change prior to final publication. Citation information: DOI 10.1109/TFUZZ.2026.3678634

Step 2: Construct two alternative, input–output equivalent TS fuzzy model representations of $\mathbf{S}(\mathbf{p})$ and the corresponding transitioning TS fuzzy model between them such that there exists convex combination of the transitioning consequent vertices that yields the non-controllable system $\mathbf{S}^{nc}(\mathbf{p})$. Specifically, execute the Double TS fuzzy model transition method (Method 5) as

$$\{\mathbf{S}(\mathbf{p}), \mathbf{S}^{nc}(\mathbf{p}), \lambda\} \xrightarrow[Type1, Type2]{\text{Double TS Transition}} \{\mathcal{S}^\lambda, \mathbf{w}_n^\lambda(p_n), \mathbf{v}_n^\lambda(p_n)\} \tag{37}$$

which results in

$$\mathbf{S}(\mathbf{p}) = \mathcal{S}^\lambda \boxtimes_{n=1}^{N} \mathbf{w}_n^\lambda(p_n) \text{ and } \mathbf{S}^{nc}(\mathbf{p}) = \mathcal{S}^\lambda \boxtimes_{n=1}^{N} \mathbf{v}_n^\lambda(p_n). \tag{38}$$

Since λ can take any value in the interval [0,1], this construction yields infinitely many TS fuzzy model representations of $\mathbf{S}(\mathbf{p})$. According to Property 1, in all these cases the LMIs $\{\mathcal{S}^\lambda\} \xrightarrow{LMI} \{\mathcal{F}\}$ are not feasible since $\mathcal{S}^\lambda$ is the vertex system of a non-controllable system $\mathbf{S}^{nc}(\mathbf{p})$. Consequnetly, we can define infinite number of TS fuzzy model representations of any given $\mathbf{S}(\mathbf{p})$ that lead to infeasible LMIs.

C. Example Illustrating the Steps of the Proof

This example explicitly applies the steps of the proof (Section IV-B) demonstrating how to construct infinitely many TS fuzzy model representations that lead to infeasible LMIs and thereby establishing their existence. Consider system matrix

$$\mathbf{S}(p) = \begin{bmatrix} 1 & 0 & 2+cos(p) \\ -1 & 2+sin(p) & 0 \end{bmatrix}. \tag{39}$$

$p = x_1 \in [0, 2\pi]$ and where $\mathbf{x} \in \mathbb{R}^2$. This simple example is chosen because only two elements, such as $[\mathbf{S}(p)]_{2,2}$ and $[\mathbf{S}(p)]_{1,3}$, of the system matrix depend on p, allowing a clear visualization, where only these two elements are shown in a two-dimensional coordinate system.

Following Step 1 of the proof (Section IV-B): We define a non-controllable system

$$\mathbf{S}^{nc}(p) = \begin{bmatrix} 1 & 0 & 0.5+cos(p)/2 \\ -1 & sin(p)/2 & 0 \end{bmatrix}. \tag{40}$$

For the sake of generality, we assume that the cause of non-controllability is unknown. For the purpose of this example, however, we explicitly reveal the underlying cause in order to verify that the system is indeed non-controllable: for $p = 2\pi$ the input submatrix $\mathbf{B}(p) = \begin{bmatrix} 0.5+cos(p)/2 & 0 \end{bmatrix}^T$ becomes the zero matrix, which implies that the system cannot be controlled when $p = 2\pi$. The systems $\mathbf{S}(p)$ and $\mathbf{S}^{nc}(p)$ are depicted in the upper two plots in Fig. 1; see the blue and red circles.

Following Step 2 of the proof (Section IV-B): We apply the Double TS fuzzy model transition method (Method 5) to derive SNNN-type (loose convex hull) and IRNO-type (tight convex hull) TS fuzzy models and the transition between them as follows:

$$\{\mathbf{S}(p), \mathbf{S}^{nc}(p), \lambda\} \xrightarrow[\text{IRNO, SNNN}]{\text{Double TS Transition}} \{\mathcal{S}^\lambda, w_i^\lambda(p), v_i^\lambda(p)\}. \tag{41}$$

The result of the Double TS fuzzy model transition is

$$\mathbf{S}(p) = \mathcal{S}^\lambda \boxtimes_{1} \mathbf{w}^\lambda(p) \text{ and } \mathbf{S}^{nc}(p) = \mathcal{S}^\lambda \boxtimes_{1} \mathbf{v}^\lambda(p). \tag{42}$$

Since this case is very simple we may use the sum operator based form as:

$$\mathbf{S}(p) = \sum_{i=1}^{3} w_i^\lambda(p)\, \mathbf{S}_i^\lambda \quad \text{and} \quad \mathbf{S}^{nc}(p) = \sum_{i=1}^{3} v_i^\lambda(p)\, \mathbf{S}_i^\lambda, \tag{43}$$

where the minimum required number of antecedent fuzzy sets is $I = 3$. For completeness, we note that in the intermediate Step 2 of the Double TS fuzzy model transition method (Method 5) the interpolation of the antecedent sets is defined (see Eq.(32) and (12)) as $\mathbf{h}^\lambda(p) = (1-\lambda)\mathbf{h}^{IRNO}(p) + \lambda\mathbf{h}^{SNNN}(p)$ to yield smooth transition.

The convex hulls of the resulting IRNO-type ($\lambda = 0$) and SNNN-type ($\lambda = 1$) TS fuzzy model representations contain both $\mathbf{S}(p)$ and the non-controllable system $\mathbf{S}^{nc}(p)$; see the yellow (IRNO) and purple (SNNN) triangles in the upper plots of Fig. 1. The lower plots present the corresponding antecedent systems of both $\mathbf{S}(p)$ and the non-controllable system $\mathbf{S}^{nc}(p)$. The colors blue, red, and yellow correspond to index $i = 1, 2, 3$ for the antecedents $w_i(p)$, $v_i(p)$, respectively. The transition (for $\lambda \in [0, 1]$) of the TS fuzzy model is illustrated in Fig. 2. The left plot depicts the convex hulls for 30 values of λ, while the right plots illustrate the transition of the correspondimg antecedent systems for both $\mathbf{S}(p)$ and the non-controllable system $\mathbf{S}^{nc}(p)$ for 10 values of λ only (for clarity).

The conclusion of this example is that infinitely many such TS fuzzy model representations of $\mathbf{S}(p)$ can be derived whose consequent vertices are also consequent vertices of the TS fuzzy model representations of the non-controllable system $\mathbf{S}^{nc}(p)$. Therefore, the LMIs applied in this case inevitably lead to infeasibility, even though the system $\mathbf{S}(\mathbf{p})$ and the vertices of its TS fuzzy model are themselves controllable. Note that infinitely many TS fuzzy model representations can also be derived that lead to feasible LMIs; see the example in Section V-C.

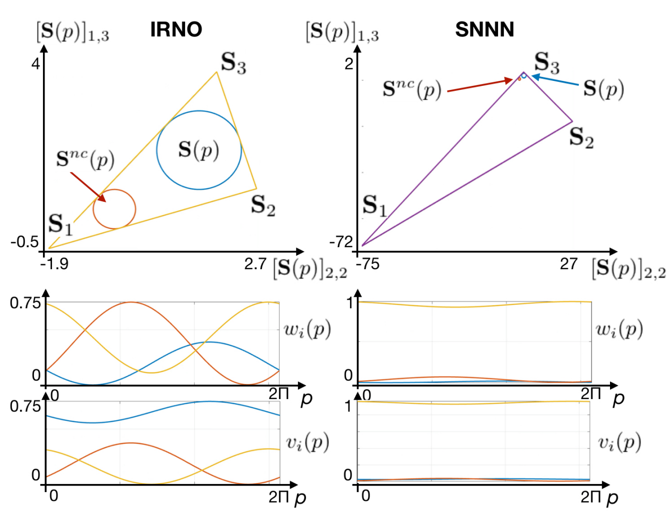

Fig. 1: SNNN and IRNO-type TS fuzzy models of $\mathbf{S}(p)$ and $\mathbf{S}^{nc}(p)$.

This article has been accepted for publication in IEEE Transactions on Fuzzy Systems. This is the author's version which has not been fully edited and content may change prior to final publication. Citation information: DOI 10.1109/TFUZZ.2026.3678634

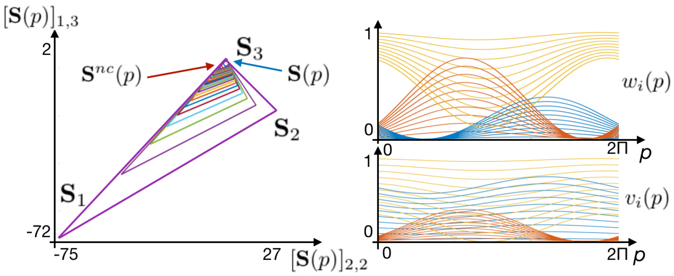

Fig. 2: Transitions between SNNN and IRNO-type TS fuzzy models of $\mathbf{S}(\mathbf{p})$ and $\mathbf{S}^{nc}(\mathbf{p})$.

V. Suboptimal LMI-Based PDC design

A. Theorem

Theorem 2: For any given system $\mathbf{S}(\mathbf{p})$ that is controllable for all $\mathbf{p}$, there exist infinitely many input–output equivalent TS fuzzy model representations whose consequent vertices define convex hulls that contain at least one controllable system $\mathbf{S}^{mc}(\mathbf{p}) \neq \mathbf{S}(\mathbf{p})$ exhibiting significantly different dynamic behavior, thereby requiring a substantially different controller under the same optimization criteria.

For ease of exposition, $\mathbf{S}^{mc}(\mathbf{p})$ may be chosen as a marginally controllable system (denoted by the superscript "mc"), i.e., it can be selected arbitrarily close to the non-controllable system $\mathbf{S}^{nc}(\mathbf{p})$. The system $\mathbf{S}^{mc}(\mathbf{p})$ may, for instance, correspond to a system whose input channel matrix $\mathbf{B}(\mathbf{p})$ is closer to zero (closer than $\mathbf{B}(\mathbf{p})$ of $\mathbf{S}(\mathbf{p})$), thereby requiring a stronger control signal to achieve the same control performance, or to a variant in which at least one row of $\mathbf{S}^{mc}(\mathbf{p})$ is closer to the corresponding row of the identity matrix. Alternatively, $\mathbf{S}^{mc}(\mathbf{p})$ may represent a variant whose controllability properties differ from those of $\mathbf{S}(\mathbf{p})$ and are closer, in some respect, to those of the non-controllable system $\mathbf{S}^{nc}(\mathbf{p})$. Thus, in general, $\mathbf{S}^{mc}(\mathbf{p})$ is, from a controllability perspective, closer to the non-controllable system $\mathbf{S}^{nc}(\mathbf{p})$ than $\mathbf{S}(\mathbf{p})$.

Practical Implication 2: If a TS fuzzy model is derived according to design considerations that do not explicitly account for what further systems are included in the convex hull of the consequents, then the resulting control solution is not guaranteed to be optimal for $\mathbf{S}(\mathbf{p})$, even though the applied LMI conditions themselves yield an optimal solution in a formal sense. Consequently, identifying an optimal controller requires the deliberate selection of antecedent fuzzy sets that induce a convex hull best aligned with the dynamics of the given system as the LMI solution inherently reflects the most weakly controllable or dynamically distant systems contained within the convex hull (see Property 1).

Consequently, contrary to common practice in the literature, practical controller synthesis should not be considered complete once a TS fuzzy model has been constructed and the LMI-based PDC framework yields a controller. Instead, it should systematically explore alternative input–output equivalent TS fuzzy model representations in order to assess whether a more favorable representation exists that leads to improved control performance.

B. Proof of Theorem 2

The proof of Theorem 2 follows the same line of reasoning as the constructive proof of Theorem 1.

Step 1: First of all let us define an $\mathbf{S}^{mc}(\mathbf{p})$.

Proposition 2: Marginally controllable systems $\mathbf{S}^{mc}(\mathbf{p})$ can always be readily constructed in the vicinity of $\mathbf{S}^{nc}(\mathbf{p})$; For example, one simple construction is to replace the input channel with a new one in which at least one element is closer to zero, as described above. In short, infinite number of such marginally controllable system $\mathbf{S}^{mc}(\mathbf{p})$ can always be constructed derived form $\mathbf{S}(\mathbf{p})$ by approaching the non-controllable system $\mathbf{S}^{nc}(\mathbf{p})$.

Step 2: Execute the Double TS fuzzy model transition method as

$$\{\mathbf{S}(\mathbf{p}), \mathbf{S}^{mc}(\mathbf{p}), \lambda\} \xrightarrow[Type1, Type2]{\text{Double TS Transition}} \{\mathcal{S}^{\lambda}, \mathbf{w}_n^{\lambda}(p_n), \mathbf{v}_n^{\lambda}(p_n)\} \tag{44}$$

which results in

$$\mathbf{S}(\mathbf{p}) = \mathcal{S}^{\lambda} \mathop{\boxtimes}_{n=1}^{N} \mathbf{w}_n^{\lambda}(p_n) \text{ and } \mathbf{S}^{mc}(\mathbf{p}) = \mathcal{S}^{\lambda} \mathop{\boxtimes}_{n=1}^{N} \mathbf{v}_n^{\lambda}(p_n). \tag{45}$$

Since λ can take any value in the interval [0,1], this construction yields infinitely many TS fuzzy model representations of $\mathbf{S}(\mathbf{p})$ whose vertices are also the vertices of $\mathbf{S}^{mc}(\mathbf{p})$. Therefore, the LMI-based design also yields (if there is no $\mathbf{S}^{nc}(\mathbf{p})$ in the convex hull) a control solution for $\mathbf{S}^{mc}(\mathbf{p})$.

Future Research Direction 1: **Controllability-Aware TS fuzzy model transformation**

The above Theorems 1 and 2 and their proof highlight that, ideally, during the derivation of the consequent vertex systems, information would be available about the location of non-controllable or marginally controllable systems within the system matrix space. Equivalently, if a controllability map of this space were known, the vertices could be derived in such a way that the resulting convex hull avoids regions associated with poor controllability, or at least remains as far as possible from them.

Some such regions are trivial and have already been mentioned — for example, cases where rows of the system matrix approach the corresponding rows of the identity matrix, or where the input channel matrix approaches zero. However, other non-controllable or only weakly controllable system variants are generally unknown, and their location within the system space is difficult to characterize.

From this perspective, the problem can be interpreted as an optimization task with respect to controllability over the convex hull defined by the TS fuzzy model. This observation forms the basis of the future research direction suggested in this paper: namely, the extension of TS fuzzy model transformation techniques to be capable of identifying convex hulls that, guided by a controllability map, predominantly encompass regions of high controllability while avoiding poorly controllable ones.

C. Illustrative example for Theorem 2 and Practical Implication 2

The primary objective of this example is to illustrate the steps of the proof of Theorem 2. In addition, the exam-

This article has been accepted for publication in IEEE Transactions on Fuzzy Systems. This is the author's version which has not been fully edited and content may change prior to final publication. Citation information: DOI 10.1109/TFUZZ.2026.3678634

ple illustrates Practical Implication 2 and demonstrates that there exist infinitely many possible selections of antecedent-consequent structure, many of which result in significantly different controllers. Consequently, one must identify, among the possible TS fuzzy model representations, the one that best achieves the desired performance.

We continue with the same system given in Eq. (39). The controller to be derived defines a gain vector $\mathbf{f}(p) \in \mathbb{R}^2$, which consists of only two elements and can therefore be conveniently visualized in a two-dimensional coordinate system.

Following Step 1 of the proof of Theorem 2 (Section V-B): Note again that if $[\mathbf{S}(p)]_{1,3} = 0$, then the system becomes uncontrollable. Let $\mathbf{S}^{mc}(\mathbf{p})$ be equal $\mathbf{S}(p)$ except elements $[\mathbf{S}^{mc}(p)]_{2,2/1,3}$ that are $[\mathbf{S}^{mc}(p)]_{2,2} = 3.5$ and $[\mathbf{S}^{mc}(p)]_{1,3} = 0.72$. In this case, the input gain $[\mathbf{S}^{mc}(p)]_{1,3}$ is closer to zero - closer to $\mathbf{S}^{nc}(p)$ - than $[\mathbf{S}(p)]_{1,3}$ for any p.

Following Step 2 of the proof of Theorem 2 (Section V-B): execute the double TS fuzzy model transition as

$$\{\mathbf{S}(p), \mathbf{S}^{mc}(p), \lambda\} \xrightarrow[CNO,SNNN]{\text{Double TS Transition}} \{\mathcal{S}^{\lambda}, \mathbf{w}^{\lambda}(p), \mathbf{v}^{\lambda}(p)\}. \tag{46}$$

The resulting infinite number of TS fuzzy model representations of $\mathbf{S}(p)$

$$\mathbf{S}(p) = \sum_{i=1}^{3} w_i^{\lambda}(p)\mathbf{S}_i^{\lambda} \tag{47}$$

has consequent vertices that are also the vertices of the TS fuzzy model representation of $\mathbf{S}^{mc}(p)$

$$\mathbf{S}^{mc}(p) = \sum_{i=1}^{3} v_i^{\lambda}(p)\mathbf{S}_i^{\lambda}. \tag{48}$$

Hence, the LMI-based PDC design yields a control solution for both $\mathbf{S}(p)$ and $\mathbf{S}^{mc}(p)$ (see Property 1), thereby potentially leading to a significant degradation of the controller optimality for $\mathbf{S}(p)$.

To illustrate how strongly the resulting controller can be influenced as $[\mathbf{S}^{mc}(p)]_{1,3}$ approaches zero, let us define a sequence of systems $\mathbf{S}_k^{mc}(p)$, $k = 1,2,3,4$, as $[\mathbf{S}_1^{mc}(p)]_{2,2/1,3} = [3.5, 0.72]$, $[\mathbf{S}_2^{mc}(p)]_{2,2/1,3} = [3.35, 0.43]$, $[\mathbf{S}_3^{mc}(p)]_{2,2/1,3} = [3.1, 0.27]$ and $[\mathbf{S}_4^{mc}(p)]_{2,2/1,3} = [3, 0.2]$. These values are then substituted into Eqs. (46). For the sake of clarity and simplicity of visualization, we consider the case $\lambda = 0$ for all k, that is, the tightest convex hull (CNO). The left plot of Fig. 3 illustrates the resulting triangular convex hulls. The colors blue, red, yellow, and purple correspond to $k = 1, 2, 3$, and 4, respectively. The antecedent sets are shown in the right plot (with the same color order). It can be observed that they are highly similar to each other. The controller gain

$$\mathbf{f}^k(p) = \sum_{1}^{3} w_i^k(p)\mathbf{f}_i^k, \tag{49}$$

is obtained by deriving the vertex gains $\mathbf{f}_i^k$ by $\{\mathbf{S}_i^k\} \xrightarrow{LMI} \{\mathbf{f}_i^k\}$ using Theorem 2. The triangular convex hulls defined by these vertices $\mathbf{f}_i$, together with the corresponding controller gain functions $\mathbf{f}(p)$, are shown for all p in blue in the left images of Fig. 4 for $k = 1$. The right plot depicts $\mathbf{f}^k(p)$ for $k = 2,3,4$, using the same color order as above (red,

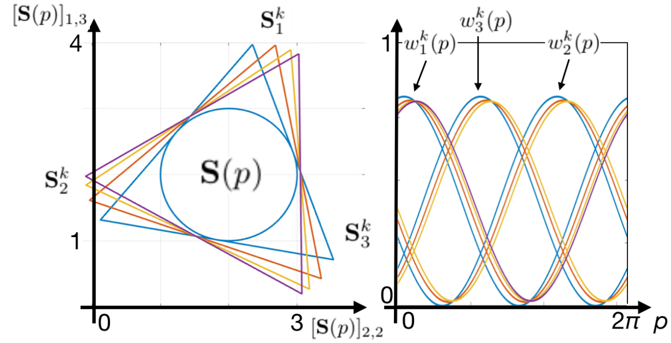

Fig. 3: TS fuzzy model vertices when $\mathbf{S}^{mc}(p)$ approaches $\mathbf{S}^{nc}(p)$.

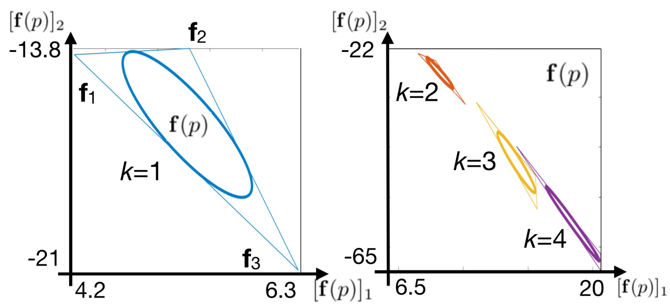

Fig. 4: TS fuzzy controller vertices when $\mathbf{S}^{mc}(p)$ approaches $\mathbf{S}^{nc}(p)$.

yellow, purple). From the vertical and horizontal axes, it can be observed that the controller gain for $k = 1$ lies in the range $[4.2, 6.3] \times [-13.8, -21]$, whereas for $k = 2,3,4$ this range increases rapidly. If a further system $\mathbf{S}^{mc}(p)$ is selected, with $[\mathbf{S}^{mc}(p)]_{1,3} = 0.1$, that is, even closer to zero, the controller gain increases substantially, reaching magnitudes on the order of 10^5. Based on the above observations, the smallest control signal is obtained for the case $k = 1$.

In summary, the figure clearly illustrates that, even though the antecedent sets differ only slightly, the resulting controllers differ significantly even when applying the same design LMIs. Moreover, the LMI-based PDC framework becomes increasingly biased toward optimizing for $[\mathbf{S}^{mc}(p)]$ as $[\mathbf{S}^{mc}(p)] \to \mathbf{S}^{nc}(p)$.

An important remark is that, in all considered cases, the tightest possible convex hull was constructed; nevertheless, the resulting solutions range from optimal to strongly suboptimal, or even infeasible control designs. This clearly demonstrates that, although it may appear as a trivial intuition that a tighter convex hull contains fewer $\mathbf{S}^{mc}(\mathbf{p})$ or no $\mathbf{S}^{nc}(\mathbf{p})$ systems and therefore leads to better solutions, this assumption does not hold in general. While tightening the convex hull may increase the likelihood of excluding $\mathbf{S}^{mc}(\mathbf{p})$ or $\mathbf{S}^{nc}(\mathbf{p})$ systems and obtaining an improved solution, it does not guarantee optimality, as the outcome fundamentally depends on the controllability properties of the systems within the convex hull. Figure 5 illustrates cases in which enlarging the convex hull (left plot) results in smaller control signals (right plot) compared to the previous cases; see the right plot in Figure 4.

This article has been accepted for publication in IEEE Transactions on Fuzzy Systems. This is the author's version which has not been fully edited and content may change prior to final publication. Citation information: DOI 10.1109/TFUZZ.2026.3678634

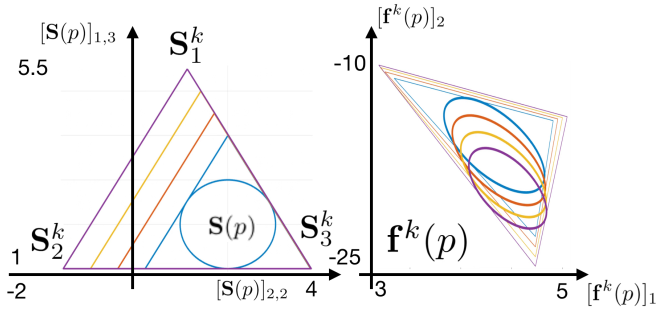

Fig. 5: TS fuzzy model and controller vertices corresponding to an enlarged convex hulls

VI. Example: A Real-World Engineering Problem

The primary objective of this real-world benchmark example is to demonstrate the theorems and the Practical Implication 2. Important point to note is that this example does not aim to identify the best possible solution according to application-specific criteria for the considered example system, which would be beyond the scope permitted by the limited length of the paper. Instead, the purpose is to demonstrate that LMI-based PDC design is highly sensitive to the selection of the applied antecedent–consequent structure. Therefore, claims of achieving the best control performance in previous papers [4], [24], [34] on this real-world benchmark problem should have been justified by demonstrating that the selected antecedent–consequent structure is optimal with respect to the considered design objectives. The present example shows that the systematic antecedent–consequent structure exploration technique developed in the proofs can lead to better results than those previously published.

Let us focus on the highly complex benchmark control design challenge of the prototypical aeroelastic wing section, where parameters of the model were identified based on real-life measurements conducted by NASA. It is also widely used in TS fuzzy model transformation-related literature, making this choice an opportunity for comparison with previous results [4], [5], [24], [25], [28], [30]. The challenge of TS fuzzy modeling and control design for this system lies in its strong non-linearities and dynamic complexity, which can even result in chaotic motion under certain conditions.

Due to the strict length limitations of this paper, we provide a brief summary of the qLPV model for the prototypical aeroelastic wing section. For further details and physical descriptions, please refer to [4], [5], [24], [25], [28], [30]. The state vector is $\mathbf{x}(t) \in \mathbb{R}^4$ and the parameter vector is $\mathbf{p}(t) = \begin{bmatrix} U(t) & x_2(t) \end{bmatrix} \in \begin{bmatrix} 14 & 25 \end{bmatrix} \times \begin{bmatrix} -0.3 & 0.3 \end{bmatrix} \subset \mathbb{R}^2$. $U(t)$ wind speed is an external parameter, $x_1(t)$ is plunging, while $x_2(t)$ is the pitching displacement of the wing. For simplicity, we will omit time t from this point forward in the example. The system matrix $\mathbf{S}(\mathbf{p}) \in \mathbb{R}^{4\times 5}$ is

$$\mathbf{S}(\mathbf{p}) = \begin{bmatrix} 0 & 0 & 1 & 0 & 0 \\ 0 & 0 & 0 & 1 & 0 \\ -k_1 & K_1(\mathbf{p}) & -c_1(U) & -c_2(U) & g_3U^2 \\ -k_3 & K_2(\mathbf{p}) & -c_3(U) & -c_4(U) & g_4U^2 \end{bmatrix}, \quad (50)$$

where the parameter dependent components are in partition $[\mathbf{S}(\mathbf{p})]_{3:4,2:5}$ as:

$$K_1(\mathbf{p}) = -k_2U^2 - p(x_2);\; K_2(\mathbf{p}) = -k_4U^2 - q(x_2); \quad (51)$$

$$p(x_2) = -0.0977k_\alpha(x_2);\; q(x_2) = 15.5020k_\alpha(x_2); \quad (52)$$

$$k_\alpha(x_2) = 2.82(1 - 22.1x_2 + 1315.5x_2^2 + 8580x_2^3 + 17289.7x_2^4); \quad (53)$$

$$c_1(U) = (I_\alpha c_h + U(I_\alpha \rho b c_{l_\alpha} + m x_\alpha \rho c_{m_\alpha}))/d; \quad (54)$$

$$c_2(U) = (z\rho U(I_\alpha b^2 c_{l_\alpha} + m x_\alpha b^4 c_{m_\alpha}) - m x_\alpha b c_\alpha)/d; \quad (55)$$

$$c_3(U) = -m(x_\alpha b c_h + \rho U b^2(x_\alpha c_{l_\alpha} + c_{m_\alpha}))/d; \quad (56)$$

$$c_4(U) = m(c_\alpha - z\rho U b^3(x_\alpha c_{l_\alpha} + c_{m_\alpha}))/d. \quad (57)$$

The constants are $a = -0.4$, $b = 0.135$, $k_h = 2844.4$, $c_h = 27.43$, $c_\alpha = 0.036$, $\rho = 1.225$, $c_{l_\alpha} = 6.28$, $c_{l_\beta} = 3.358$, $c_{m_\alpha} = (0.5 + a)c_{l_\alpha}$, $m = 12.387$, $c_{m_\beta} = -0.635$, $x_\alpha = -0.3533 - a$, $I_\alpha = 0.065$, $d = 0.7991$, $k_1 = 231.3804$, $k_2 = 0.0859$, $k_3 = -277.9906$, $k_4 = -0.3188$, $g_3 = -0.0438$, $z = (1/2 - a)$ and $g_4 = -0.1655$.

A. Demonstrating Theorem 1 and Practical Implication 1 on Feasibility

This section demonstrates that there are infinitely many "good" and "bad" selections of the antecedent system and the associated convex hull in the present example, leading to either feasible or infeasible designs. It is difficult to distinguish between them without deeper analysis to determine why those lead to a feasible design. This underscores the critical importance of searching for an appropriate antecedent-consequent structure.

Following the standard steps of the LMI-based PDC design procedure, we first derive a TS fuzzy model of $\mathbf{S}(\mathbf{p})$, then we apply LMIs to derive the controller feedbacks. In principle, this can be accomplished by an arbitrary modeling technique, for instance by analytically deriving it from Eqs. (51–57) (which in the present case would be overly complicated) or by applying a general approach such as the sector nonlinearity method. However, due to the complexity of the system, we execute the TS fuzzy model transformation here, which is preferred here because of its fast, fully numerical, and automatic execution.

Accordingly, for the considered model Eq. (50) we apply the TS fuzzy model transformation (Method 1)

$$\{\mathbf{S}(\mathbf{p})\} \xrightarrow[Type]{\text{TS Transformation}} \{\mathcal{S},\ \mathbf{w}_n(p_n)\} \quad (58)$$

where $Type \in \{SNNN, IRNO\}$. In the present case, the transformation is exact, i.e., it yields input–output equivalent TS fuzzy models:

$$\mathbf{S}(\mathbf{p}) = \mathcal{S}^{Type} \mathop{\boxtimes}_{n=1}^{2} \mathbf{w}_n^{Type}(p_n), \quad (59)$$

where $\mathcal{S}^{Type} \in \mathbb{R}^{3\times 2\times 4\times 5}$, $\mathbf{w}_1^{Type}(p_1) \in \mathbb{R}^3$, $\mathbf{w}_2^{Type}(p_2) \in \mathbb{R}^2$. Hence, along the first dimension three, and along the second dimension two antecedent fuzzy sets are the minimum required to obtain an exact TS fuzzy model representation. In

This article has been accepted for publication in IEEE Transactions on Fuzzy Systems. This is the author's version which has not been fully edited and content may change prior to final publication. Citation information: DOI 10.1109/TFUZZ.2026.3678634

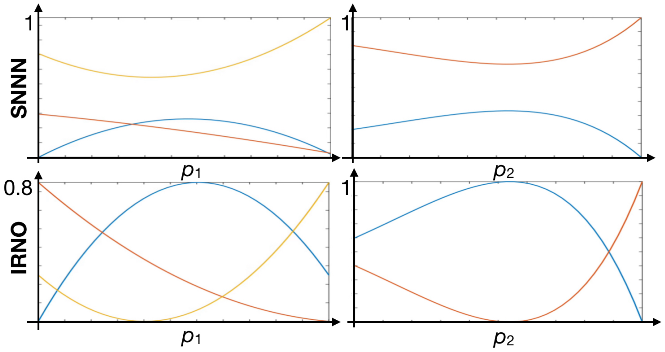

Fig. 6: SNNN- and IRNO-type antecedent fuzzy sets.

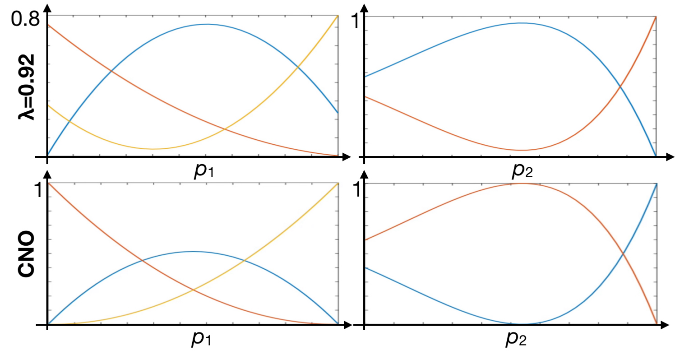

Fig. 7: Antecedent fuzzy sets for $\lambda = 0.92$ and CNO-type antecedent fuzzy sets.

classical product-summation form Eq. (3), this representation can be written as

$$\mathbf{S}(p_1, p_2) = \sum_{i_1=1}^{I_1=3} \sum_{i_2=1}^{I_2=2} w_{1,i_1}^{Type}(p_1) w_{2,i_2}^{Type}(p_2) \mathbf{S}_{i_1,i_2}^{Type}, \quad (60)$$

where $\mathbf{S}_{i_1,i_2}^{Type} = [\mathcal{S}^{Type}]_{i_1,i_2}$ and $\mathbf{S}_{i_1,i_2}^{Type} \in \mathbb{R}^{4\times5}$. The antecedent fuzzy sets are depicted in Fig. 6. The blue, red, and yellow colors correspond to the indices $i = 1, 2, 3$ of $w_{n,i_n}(p_n)$, respectively.

Reflecting Practical Implication 1: If the consequents of both the input–output equivalent SNNN- and IRNO-type TS fuzzy models are substituted into the LMIs of Theorem 2 then markedly different outcomes are obtained. For the SNNN-type representation the resulting LMIs are infeasible. In contrast, for the IRNO-type representation the LMIs are feasible and the corresponding controller can be successfully derived.

In the remainder of this section, we derive infinitely many further antecedent-consequent structures by applying the transition techniques used in the proof, and investigate whether TS fuzzy models constructed "between" the SNNN and IRNO representations yield feasible LMI-based PDC control designs, thereby providing further candidate controllers.

Case A: A transition is defined from the SNNN-type TS fuzzy model to the IRNO-type TS fuzzy model by Method 3:

$$\{\mathcal{S}^{SNNN}, \mathbf{w}_n^{SNNN}(p_n), \mathcal{S}^{IRNO}, \mathbf{w}_n^{IRNO}(p_n), \lambda, \} \quad (61)$$
$$\xrightarrow{\text{TS Transition}} \{\mathcal{S}^{\lambda}, \mathbf{w}_n^{\lambda}(p_n)\}$$

In the present case, the antecedent system is defined as $\mathbf{w}_n^{\lambda}(p_n) = (1-\lambda)\mathbf{w}_n^{SNNN} + \lambda \mathbf{w}_n^{IRNO}$ for all $\lambda \in [0, 1]$ which yields a smooth transition between the two TS fuzzy model representations. For later visualization, we note that the original system model contains parameter-dependent elements only in the submatrix $[\mathbf{S}_{i_1,i_2}]_{3:4,2:5}$ (see Eq. (50)) and consequently the vertex systems - derived by the TS fuzzy model transformation and transition - differ exclusively in the corresponding submatrix of the vertices $[\mathbf{S}^{\lambda}_{i_1,i_2}]_{2:4,2:5}$.

Since the values of these vertex elements span vastly different ranges in respect of λ, we display them in four separate ranges, shown in the four upper plots of the left column of Fig. 8, in order to improve clarity. The plots illustrate the behavior of the vertex elements and reveal the clear tendency that, as λ increases, the values of the vertex elements become confined

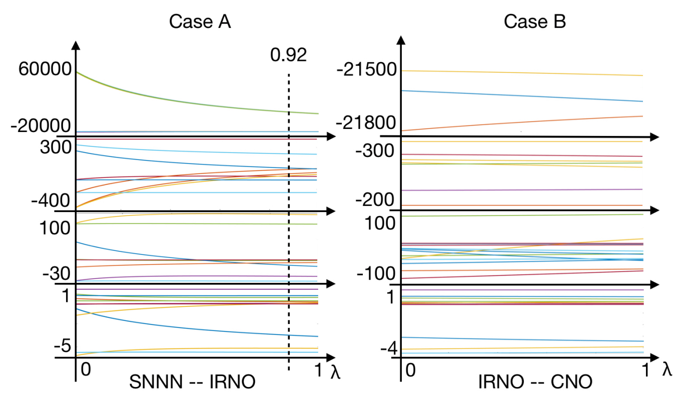

Fig. 8: Different TS fuzzy model transitions

to an increasingly narrower range. Consequently, the convex hull defined by the vertices becomes progressively tighter. In connection with Practical Implication 1, if for each value of λ the vertices of the corresponding TS fuzzy model are substituted into the same set of LMIs (Theorem 2), it can be observed that the LMIs are feasible for $\lambda \geq 0.92$ and infeasible for $\lambda < 0.92$. This implies that, for $\lambda \geq 0.92$, the corresponding convex hulls avoid any possible $\mathbf{S}^{nc}(\mathbf{p})$. The antecedent fuzzy sets $w^{\lambda}_{n,i_n}(p_n)$ for $\lambda = 0.92$ are depicted in the upper plot of Fig. 7.

Note that, without a deeper analysis — in particular, without constructing the controllability (or feasibility) map over the entire space of possible convex hulls — the locations of all $\mathbf{S}^{nc}(\mathbf{p})$ systems are not known a priori. Therefore, it is difficult to determine what type of convex hull would exclude all possible $\mathbf{S}^{nc}(\mathbf{p})$.

B. Demonstrating Theorem 2 and Practical Implication 2 on optimal solution

When, in the previous section, we derived TS fuzzy model that led to feasible LMIs (for instance when $\lambda = 0.92$) and thus enabled the derivation of a controller, the design would be regarded as complete in the literature employing the LMI-based PDC design framework, since a stabilizing controller optimized via the LMIs is already available.

However, Theorem 2 and Practical Implication 2 of the present paper point out that it is worthwhile to further search

This article has been accepted for publication in IEEE Transactions on Fuzzy Systems. This is the author's version which has not been fully edited and content may change prior to final publication. Citation information: DOI 10.1109/TFUZZ.2026.3678634

for more favorable convex hulls and to select, from the resulting set of controllers, the one that best meets the desired control performance.

To this end, we derive the controllers using Theorem 2 for all TS fuzzy models obtained from Eq. (61) with $\lambda \geq 0.92$ and we investigate how the resulting controller gains

$$\mathbf{f}(p_1, p_2) = \sum_{i_1=1}^{3} \sum_{i_2=1}^{2} w_{1,i_1}^{\lambda}(p_1) w_{2,i_2}^{\lambda}(p_2) \mathbf{f}_{i_1,i_2}^{\lambda} \qquad (62)$$

vary with respect to λ. Depicting the location of the vertices of TS Fuzzy controller would require a four-dimensional geometric plot. Therefore, instead, two figures are presented: one illustrates the values of the elements of the vertices as a function of λ, and the other shows the surface of the elements of the gain vector $\mathbf{f}(\mathbf{p})$ as functions of $\mathbf{p}$. The three plots in the left column of Figure 9 show the values of the elements of the resulting controller vertices $[\mathbf{f}_{i_1,i_2}^{\lambda}]_{1:4}$ for all i_1, i_2 as functions of λ. Each plot depicts the values of the controller vertices over different ranges for clarity. The plots clearly show that the values become confined to progressively narrower ranges as λ increases. Thus, in the present case, tightening the convex hull defined by the consequent vertices of the TS fuzzy model also leads to a tightening of the convex hull of the feedback vertices of the resulting controller.

Fig. 10 shows four plots, each depicting one element of $\mathbf{f}^{\lambda}(p_1, p_2)$ for $\lambda = 0.92$, for an intermediate value $\lambda = 0.95$, and for $\lambda = 1$ (which corresponds to the IRNO-type convex hull). It can be clearly seen from the Fig. 10 that the control gains $\mathbf{f}(\mathbf{p})$ differ - decrease in the present case - significantly. At the same time, the corresponding antecedent fuzzy sets shown in the lower plot of Fig.6 and in the upper plot of Fig.7 are almost identical. This observation directly supports the message of Practical Implication2.

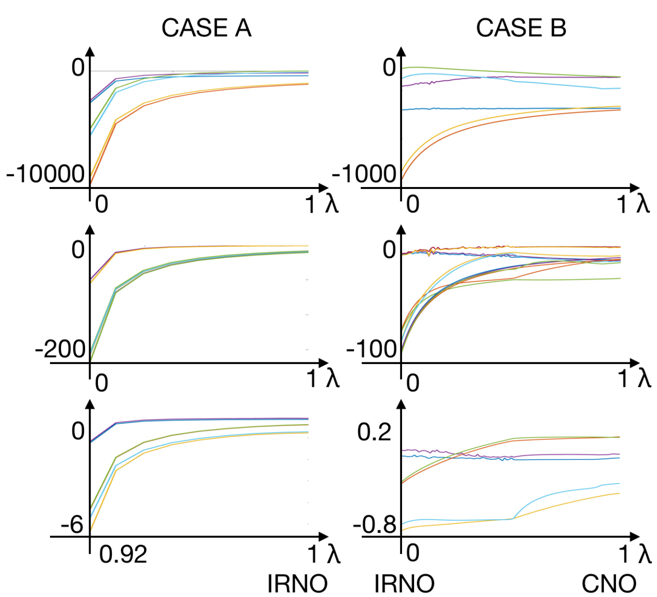

Fig. 9: Elements of the controller vertices as function of λ

Motivated by Practical Implication 2, let us further explore additional TS fuzzy model representations. To this end, we execute the TS fuzzy model transformation again, as in Eq. (58), but now derive a CNO-type (tight convex hull) TS fuzzy model. The antecedent fuzzy sets are depicted in the lower plot of Fig. 7. The resulting vertex systems lead to feasible LMIs of Theorem 2.

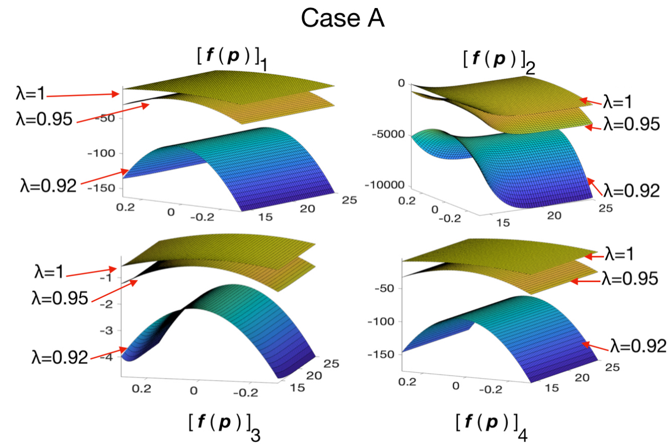

Fig. 10: Controller gains $\mathbf{f}(\mathbf{p})$ during the transition from SNNN to IRNO for given λ. The vertical axes represent the control gains. The "horizontal" axes, ranging over $\begin{bmatrix} 14 & 25 \end{bmatrix}$, correspond to p_1, while the additional axes, ranging over $\begin{bmatrix} -0.3 & 0.3 \end{bmatrix}$, correspond to p_2.

Case B: let the transition from IRNO-type TS fuzzy model to CNO-type be investigated by Method 3 as

$$\{\mathcal{S}^{IRNO}, \mathbf{w}_n^{IRNO}(p_n), \mathcal{S}^{CNO}, \mathbf{w}_n^{CNO}(p_n), \lambda, \} \qquad (63)$$
$$\xrightarrow{\text{TS Transition}} \{\mathcal{S}^{\lambda}, \mathbf{w}_n^{\lambda}(p_n)\}$$

The antecedent system is interpolated (in order to determine smooth transition the antecedents are swapped) as $\mathbf{w}_1^{\lambda}(p_1) = (1-\lambda)\mathbf{w}_1^{IRNO}(p_1) + \lambda[\mathbf{w}_1^{CNO}(p_1)]_{3,1,2}$ and $\mathbf{w}_2^{\lambda}(p_2) = (1-\lambda)\mathbf{w}_2^{IRNO}(p_2) + \lambda[\mathbf{w}_2^{CNO}(p_2)]_{2,1}$. The values of the resulting vertex elements are shown in the right column of plots in Fig. 8. Again, for clarity, the values are classified into four ranges and depicted in four separate plots. It can be observed that the values become confined to a slightly narrower range; thus, the convex hull tightens further, albeit only moderately.

Next, we derive TS fuzzy controllers for all the TS fuzzy models obtained in Eq.(63) for all λ using the same LMIs (Theorem 2). The goal of this investigation is to provide an opportunity to select an even more favorable TS fuzzy controller. We find that all these TS fuzzy model representations lead to feasible LMIs.

The three plots in the right column of Figure 9 show the values of the elements of the resulting controller vertices $[\mathbf{f}_{i_1,i_2}^{\lambda}]_{1:4}$ for all i_1, i_2 as functions of λ. Again, each plot depicts the values of the controller vertices over different ranges. The plots clearly show that the values become confined to progressively narrower ranges as λ increases. Again, in the present case, tightening the convex hull defined by the consequent vertices of the TS fuzzy model also leads to a tightening of the convex hull of the feedback vertices of the resulting controller. Similarly to the previous Case A, Fig. 11 shows the elements of $\mathbf{f}^{\lambda}(\mathbf{p})$ for all $\mathbf{p}$ in Case B. Again,

This article has been accepted for publication in IEEE Transactions on Fuzzy Systems. This is the author's version which has not been fully edited and
content may change prior to final publication. Citation information: DOI 10.1109/TFUZZ.2026.3678634

each plot corresponds to one element of the four-dimensional feedback vector $\mathbf{f}(\mathbf{p})$. For clarity of visualization, only three values of λ are selected: $\lambda = 0$, which corresponds to the IRNO-type TS fuzzy model, an intermediate value $\lambda = 0.5$, and finally $\lambda = 1$, which corresponds to the CNO-type TS fuzzy model.

It can be clearly observed in Fig. 11 that different controller gains are obtained again. The difference is significant between the cases $\lambda = 0$ and $\lambda = 1$. At the same time, the corresponding antecedent fuzzy sets shown in the lower plots of Fig.6 and Fig.7 are highly similar. This observation directly supports the message of Practical Implication2.

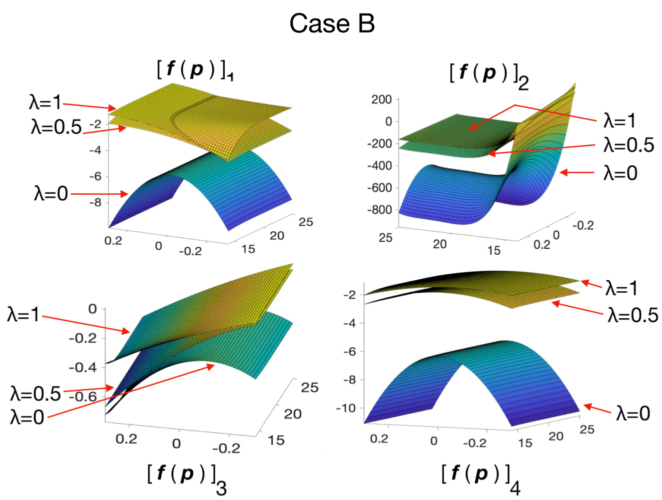

Fig. 11: Controller gains $\mathbf{f}(\mathbf{p})$ during the transition from IRNO to CNO for given λ. The vertical axes represent the control gains. The "horizontal" axes, ranging over $\begin{bmatrix}14 & 25\end{bmatrix}$, correspond to p_1, while the additional axes, ranging over $\begin{bmatrix}-0.3 & 0.3\end{bmatrix}$, correspond to p_2.

C. Comparative Analysis of Closed-Loop Pole Locations for the Derived Controllers

Due to the limited length of the paper, only three controllers are compared. The first one — Controller 1 — is the controller obtained in Case A for $\lambda = 0.92$. Controllers 2 and 3 correspond to the controllers derived from the IRNO-type and CNO-type TS fuzzy model representations, respectively.

The open-loop and the resulting closed-loop pole maps are shown in Fig.12, while a zoomed-in view of the same pole map is presented in Fig.13. The pole maps depicts the poles for all values of $\mathbf{p}$ (over a rectangular equidistant grid in Ω).

In the present case, the system has four poles. The open-loop system exhibits two complex-conjugate pole pairs, as indicated by the red circles. For Controllers 1 and 2, the closed-loop system has one complex-conjugate pair and two real poles located on the real axis. In contrast, for Controller 3, the number of real and complex poles alternates with the parameter $\mathbf{p}$: the system exhibits either two real poles and one complex-conjugate pair, or two complex-conjugate pole pairs.

It can be observed that the Controllers 1,2 and 3 lead to significantly different closed-loop pole locations, which in turn result in substantially different control performance. Thus, one must select the controller that best fits the desired control performance.

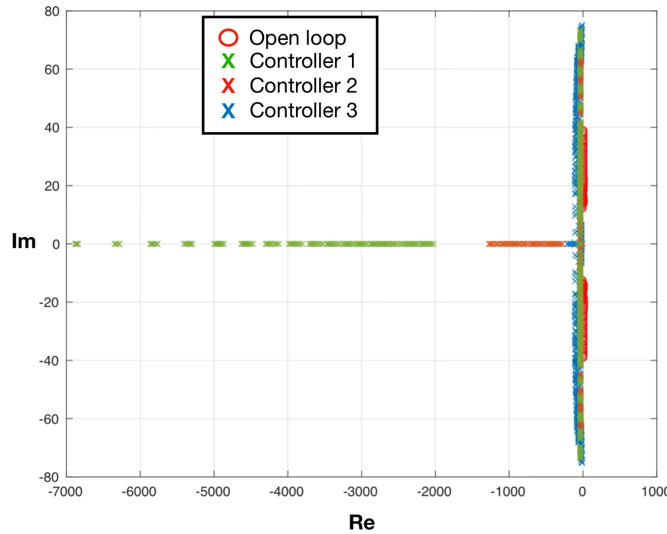

Fig. 12: Comparison of Closed-Loop Pole Maps

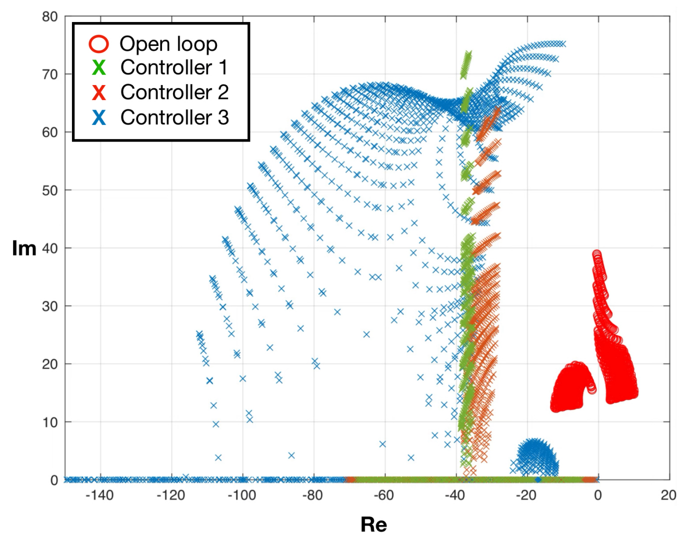

Fig. 13: Comparison of Closed-Loop Pole Maps (Zoomed-In View)

D. Simulation results

The objective of this section, in accordance with Practical Implication 2, is to demonstrate that the controllers derived above yield significantly different control signals in the numerical simulation.

Figure 14 presents the system simulation results. The figure contains six plots. All plots share a time axis spanning from 0s to 3.5s except for the plot in the middle-right position, which provides a zoomed-in view of the interval from 0s to 0.004s. The upper-left plot depicts the disturbance, expressed in degrees $(^\circ)$, applied to the control signal. The upper-right plot shows the external parameter p_2, corresponding to the

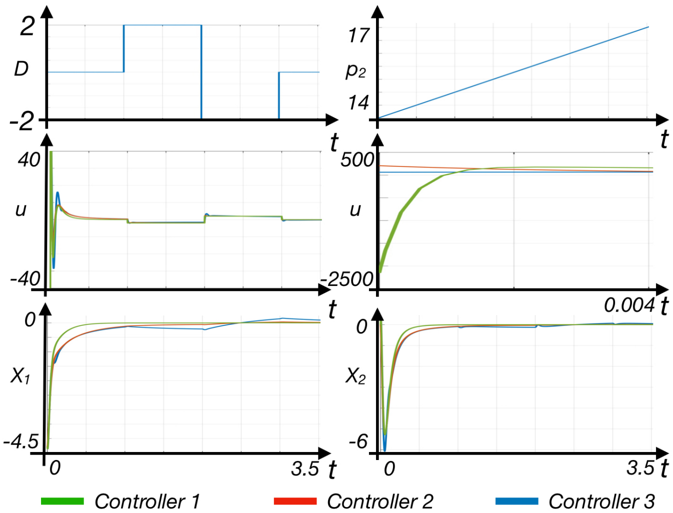

Fig. 14: Simulation results

wind speed, which varies between $14\mathrm{m/s}$ and $17\mathrm{m/s}$ — a range known to be particularly critical (could lead to chaotic behaviour) for the system's behavior.

The middle-left plot illustrates the control signal, while the middle-right plot presents a zoomed-in view of this signal. The lower-left plot shows the plunge displacement x_1 in millimeters, whereas the lower-right plot depicts the pitch angle x_2 (that is p_2) in degrees (°). In all cases, the state variables are successfully regulated from $\mathbf{x}(0) = \begin{bmatrix}0 & -0.075 & 0 & 0\end{bmatrix}$ to zero, exhibiting sufficiently similar performance. Nevertheless, it can be clearly observed that the control signals differ substantially across the controllers, a behavior already indicated by the pole maps in Figs. 12 and 13.

Controller 1 produces noticeably larger control signals than the others, reaching amplitudes that are too high for realistic implementation. Controller 2 (IRNO-type) yields considerably lower control effort, although the signal magnitude remains relatively high from a practical standpoint. In contrast, Controller 3 (CNO-type) produces the smallest control signal at $t = 0, \mathrm{s}$, which is advantageous from an implementation perspective; however, it leads to overshoots — see the blue peak in the middle plot of the left column of Fig. 14 — and the state x_1 is less effectively controlled — see the blue curve in the bottom plot of the left column. Consequently, Controller 3 exhibits the slowest response among the considered controllers. These characteristics are already clearly reflected in the closed-loop pole maps presented in the previous section.

These observations suggest that a favourable trade-off between response speed and control effort can be achieved by selecting a controller associated with an intermediate antecedent–consequent structure, lying between Controllers 2 and 3, which can be conveniently tuned by adjusting λ in Eq. (63).

E. Conclusion of the real-world example

All the above investigations of the real-world example illustrate that there are infinitely many TS fuzzy model representations of a given system, with some leading to feasible LMIs and significantly different controllers, and others to infeasible LMIs within the same LMI-based PDC controller design. If we compare the antecedent fuzzy sets obtained for $\lambda = 0.92$ and the IRNO- and CNO-type antecedents, we can observe that they are highly similar; however, the resulting controllers differ significantly. Consequently, selecting an antecedent-consequent structure without systematic further exploration of choices is more akin to a matter of chance than a systematic approach, making it uncertain whether it will yield feasible LMIs and an optimal or most effective control feedback gain. Therefore, exploring of a proper antecedent-conseuqent structure is crucial to achieve optimal control design.

The significance of this is further reinforced by the fact that, in the present example, earlier publications report results obtained using the CNO-type convex hull, whereas — as demonstrated above — superior performance can be achieved at different intermediate configurations along the transition between IRNO and CNO. In this way, solutions can be selected that are also appropriate from an engineering perspective.

VII. Conclusion

This paper has established that the selection of the antecedent–consequent structure in a TS fuzzy model is a decisive factor in the feasibility and optimality of LMI-based PDC control design framework. A key theoretical outcome of the paper is that a controller synthesized via an LMI-based PDC framework cannot be regarded as definitive or optimal unless it is verified that a suitably chosen antecedent–consequent structure has been employed.

From a practical perspective, the results clearly indicate that this sensitivity to antecedent–consequent structure selection is not an artifact of specific examples, but rather an inherent property of all qLPV systems. Consequently, the conservatism and potential suboptimality commonly associated with LMI-based PDC control design cannot be attributed solely to the LMI formulations themselves; they must also be understood as a direct consequence of how the antecedent–consequent structure of the TS fuzzy model representation is derived. The theoretical findings have been supported by both geometrically interpretable conceptual examples and a dynamically complex real-world benchmark example, demonstrating that the identified phenomena are not only theoretically relevant but also of practical significance.

The paper does not introduce a new control design method. However, the transition method developed within the proofs and applied in the examples provides a first-order solution for systematically exploring antecedent–consequent structures. The paper demonstrates, through a real-world benchmark problem, that by applying this transition method, improved solutions can be achieved compared to those reported in previous publications. Furthermore, this transition method may serve as a theoretical foundation for future research aimed at developing even more advanced exploration strategies for antecedent–consequent structures, with the goal of reducing conservatism and improving achievable control performance in TS fuzzy model–based PDC design.

REFERENCES

[1] K. Tanaka and H. Wang, *Fuzzy control systems design and analysis: a linear matrix inequality approach*. John Wiley and Sons, Inc., U.S.A., 2001.

[2] C. Scherer and S. Weiland, "Linear matrix inequalities in control," *Lecture Notes, Dutch Institute for Systems and Control, Delft, The Netherlands*, 2000, http://www.cs.ele.tue.nl/sweiland/lmi.htm.

[3] P. Baranyi, "Transition between TS Fuzzy models and the associated convex hulls by TS Fuzzy model transformation," *IEEE Transactions on Fuzzy Systems*, vol. 32, no. 4, pp. 2272–2282, 2024.

[4] P. Baranyi, *TP-Model Transformation Based Control Design Frameworks*, ser. Control Engineering. Springer book, July 2016, ISBN 978-3-319-19605-3.

[5] A. Szollosi and P. Baranyi, "Influence of the tensor product model representation of qLPV models on the feasibility of linear matrix inequality," *Asian Journal of Control*, vol. 18, no. 4, pp. 1328–1342, 2015.

[6] A. Szollosi and P. Baranyi, "Improved control performance of the 3-dof aeroelastic wing section: a TP model based 2d parametric control performance optimization," *Asian Journal of Control*, vol. 19, no. 2, pp. 450–466, 2016.

[7] A. Szollosi and P. Baranyi, "Influence of the tensor product model representation of qLPV models on the feasibility of linear matrix inequality based stability analysis," *Asian Journal of Control*, vol. 10, no. 1, pp. 531–547, 2017.

[8] Y. Qui, J. H. Park, Park, C. Hua, and X. Wang, "Stability analysis of time-varying delay t–s fuzzy systems via quadratic-delay-product method," *IEEE Transactions on Fuzzy Systems*, vol. 31, no. 1, pp. 129–137, January 2023.

[9] A. Ait Ladel, A. Benzaouia, R. Outbib, and M. Ouladsine, "Integrated state/fault estimation and fault-tolerant control design for switched t–s fuzzy systems with sensor and actuator faults," *IEEE Transactions on Fuzzy Systems*, vol. 30, no. 8, pp. 3211–3223, 2022.

[10] Z. Sheng, C. Lin, B. Chen, and Q.-G. Wang, "Stability and stabilization of t–s fuzzy time-delay systems under sampled-data control via new asymmetric functional method," *IEEE Transactions on Fuzzy Systems*, vol. 31, no. 9, pp. 3197–3209, 2023.

[11] M. S. Aslam, P. Tiwari, H. M. Pandey, and S. S. Band, "Observer-based control for a new stochastic maximum power point tracking for photovoltaic systems with networked control system," *IEEE Transactions on Fuzzy Systems*, vol. 31, no. 6, pp. 1870–1884, 2023.

[12] Q. Lv and S. Fang, "A stability analysis method for high-speed magnetically suspended rotors based on tensor product model transformation," *IEEE Transactions on Transportation Electrification*, vol. 11, no. 2, pp. 5201–5210, 2025.

[13] B.-S. Chen, Y.-Y. Tsai, and M.-Y. Lee, "Robust decentralized formation tracking control for stochastic large-scale biped robot team system under external disturbance and communication requirements," *IEEE Transactions on Control of Network Systems*, vol. 8, no. 2, pp. 654–666, 2021.

[14] H.-Y. Sun, H.-G. Han, J. Sun, H.-Y. Yang, and J.-F. Qiao, "Security control of sampled-data t–s fuzzy systems subject to cyberattacks and successive packet losses," *IEEE Transactions on Fuzzy Systems*, vol. 31, no. 4, pp. 1178–1188, 2023.

[15] Y. Wang, S. Xu, and C. K. Ahn, "Finite-time composite antidisturbance control for t–s fuzzy nonhomogeneous markovian jump systems via asynchronous disturbance observer," *IEEE Transactions on Fuzzy Systems*, vol. 30, no. 11, pp. 5051–5057, 2022.

[16] S. Tiko and F. Mesquine, "Constrained control for a class of ts fuzzy systems," *IEEE Transactions on Fuzzy Systems*, vol. 31, no. 1, pp. 348–353, 2023.

[17] B. Visakamoorthi, P. Muthukumar, and H. Trinh, "Reachable set estimation for t–s fuzzy markov jump systems with time-varying delays via membership function dependent h performance," *IEEE Transactions on Fuzzy Systems*, vol. 30, no. 11, pp. 4980–4990, 2022.

[18] J. Hu, X. Sun, M. Zhang, and P. Shi, "An offline fuzzy model-predictive control approach using cache," *IEEE Transactions on Fuzzy Systems*, vol. 30, no. 10, pp. 4504–4514, 2022.

[19] Y. Wang, C. Hua, and P. Park, "A generalized reciprocally convex inequality on stability and stabilization for t–s fuzzy systems with time-varying delay," *IEEE Transactions on Fuzzy Systems*, vol. 31, no. 3, pp. 722–733, 2023.

[20] Y. Ren, D.-W. Ding, Q. Li, and X. Xie, "Static output feedback control for t–s fuzzy systems via a successive convex optimization algorithm," *IEEE Transactions on Fuzzy Systems*, vol. 30, no. 10, pp. 4298–4309, 2022.

[21] W. Chen, Z. Fei, X. Zhao, and M. V. Basin, "Generic stability criteria for switched nonlinear systems with switching-signal-based lyapunov functions using takagi–sugeno fuzzy model," *IEEE Transactions on Fuzzy Systems*, vol. 30, no. 10, pp. 4239–4248, 2022.

[22] Y. Kang, L. Yao, and H. Wang, "Fault isolation and fault-tolerant control for takagi–sugeno fuzzy time-varying delay stochastic distribution systems," *IEEE Transactions on Fuzzy Systems*, vol. 30, no. 4, pp. 1185–1195, 2022.

[23] Y. Yam, P. Baranyi, and C. Yang, "Reduction of fuzzy rule base via singular value decomposition," *IEEE Transactions on Fuzzy Systems*, vol. 7, no. 2, pp. 120—132, April 1999.

[24] P. Baranyi, Y. Yam, and P. Várlaki, *Tensor Product Model Transformation in Polytpic Model Based Control*, ser. Automation and Control Engineering. CRC Press, Taylor & Frances Group, March 2017, ISBN 9781138077782 - CAT K34341.

[25] P. Baranyi, *Dual-Control-Design TP and TS Fuzzy Model Transformation Based Control Optimisation and Design*, ser. Topics in Intelligent Engineering and Informatics (TIEI, volume 17). Springer book, December 2023.

[26] L. De Lathauwer, B. De Moor, and J. Vandewalle, "A multilinear singular value decomposition," *SIAM Journal on Matrix Analysis*, vol. 21, no. 4, pp. 1253–1278, 2000.

[27] P. Baranyi, "TP model transformation as a way to LMI-based controller design," *IEEE Transactions on Industrial Electronics*, vol. 51, no. 2, pp. 387–400, 2004.

[28] P. Baranyi, "The generalized TP model transformation for T–S fuzzy model manipulation and generalized stability verification," *IEEE Transactions on Fuzzy Systems*, vol. 22, no. 4, pp. 934–948, 2014.

[29] P. Baranyi, "Extracting LPV and qLPV structures from state-space functions: A TP model transformation based framework," *IEEE Transactions on Fuzzy Systems*, vol. 28, no. 3, pp. 499–509, 2020.

[30] P. Baranyi, "How to vary the input space of a T–S fuzzy model: A TP model transformation-based approach," *IEEE Transactions on Fuzzy Systems*, vol. 30, no. 2, pp. 345–356, 2022.

[31] P. Baranyi, "Relaxed TS fuzzy model transformation to improve the approximation accuracy/complexity tradeoff and relax the computation complexity," *IEEE Transactions on Fuzzy Systems*, vol. 32, no. 9, pp. 5237–5247, 2024.

[32] P. Várkonyi, D. Tikk, P. Korondi, and P. Baranyi, "A new algorithm for RNO-INO type tensor product model representation," in *Proceedings of the 9th IEEE International Conference on Intelligent Engineering Systems*, 2005, pp. 263–266.

[33] D. Tikk, P. Baranyi, and R. Patton, "Approximation properties of TP model forms and its consequences to TPDC design framework," *Asian Journal of Control*, vol. 9, no. 3, pp. 221–231, 2008.

[34] P. Baranyi, "Tensor product model based control of two dimensional aeroelastic system," *Journal of Guidance, Control and Dynamics*, vol. 29, no. 2, pp. 391–400, 2006.